University of Siena – Department of Medical Biotechnologies

Doctorate in Genetics, Oncology and Clinical Medicine (GenOMeC)

XXXIII cycle (2017-2020)

Coordinator: Prof. Francesca Ariani

Brain microsurgery in glioblastoma mouse models for local administration of Temozolomide-loaded hydrogels

Scientific disciplinary sector: MED/06 – Medical Oncology

Tutor

Dr. Chiariello Mario

Cotutor

Dr.ssa Gherardini Lisa

PhD Candidate

Francesca Dapporto

Academic Year 2019/2020

Abstract

Glioblastoma is the most common and aggressive malignant tumor of the central nervous system in adults. It can occur at any age, but 70% of patients are diagnosed between the ages of 45 and 70. These tumors show a high proliferation rate with diffuse infiltration of adjacent brain tissue and a rapidly progressive course (around 2-3 months).Tumors are usually located in the cerebral hemispheres, but can be found throughout the central nervous system. The first choice treatment is usually surgical, both to confirm the diagnosis through a biopsy, and to remove the tumor mass as extensively as possible. Unfortunately, a complete resection is very infrequent, as cancer cells usually infiltrate the surrounding brain. Therefore, the goal of surgery is only to obtain a histological diagnosis, decrease the symptoms due to the increase in intracranial pressure and prolong survival. Surgery is usually followed by radiation therapy and chemotherapy but there is a treatment gap of 2 to 3 weeks between tumor resection and subsequent therapies. The post-surgical therapeutic standard currently consists of a chemo-radiotherapy association with Temozolomide (TMZ) for the entire duration of radiotherapy, followed by adjuvant TMZ. However, tumor recurrences due to residual infiltrative cells at the resection margin are extremely common.

This study aims at developing a mouse model of glioblastoma recurrences by a surgical protocol of partial tumor removal in mouse brains, for subsequent on-site treatment with thermogel, a “smart” material loaded with TMZ. For this purpose, the U87MG human glioblastoma cell line was chosen for the development of a mouse orthotopic model in the striatum, a subcortical region of the brain. Once tumors of sufficient size were obtained, a microsurgery protocol with craniotomy was optimized for the partial removal of the tumor mass in order to study the phenomenon of recurrence. The cavity thus obtained was filled with thermogel containing TMZ. The effect due to this treatment was confirmed by two different types of analysis: histological and bioluminescent. The histological analysis allowed us to verify the correct inoculation region of the tumor cells and to verify their growth. Furthermore, by measuring the tumor present in the brain slices removed from treated and untreated mice, we were able to measure the area of

each tumor with a specific software, verifying the effectiveness of the treatment. To confirm obtained data, we carried out another type of analysis, using the IVIS In Vivo Imaging System, usingU87MG cells stably expressing the firefly enzyme luciferase from *Luciola Italica* (Red-FLuc). By recording the bioluminescence emitted by the tumor cells inoculated inside the brain of the mice, following an adequate stimulus, we confirmed the effect of the treatment of the thermogel containing the chemotherapeutic.

Introduction

Glioblastoma

Glioblastoma multiforme (GBM) is the most common and lethal malignant tumor among glia neoplasms, comprising 16% of all primary brain and central nervous system cancers **(Thakkar et al., 2014)**. These tumors make up about half of all astrocytomas and they can occur at any age, but are more common in adult patients. GBM is a grade IV glioma, which is the most aggressive form, and shows a high proliferation rate with diffuse infiltration of adjacent brain tissue. Its invasive growth pattern makes a complete surgical resection nearly impossible. Furthermore, the drugs administered must be able to pass the blood-brain barrier. Despite aggressive treatment including surgical resection, chemo- and radiotherapy, tumor recurrences due to residual cells at the resection margin are inevitable leading to a median survival of about 14.6 months **(Stupp et al., 2005)** with a 5 year-life expectancy of less than 5%. Median survival is generally less than one year from the time of diagnosis, and even in the most favorable situations, most patients die within two years.

Due to its high degree of invasiveness, radical resection of the primary tumor mass is not curative. In fact, infiltrating tumor cells invariably remain within the surrounding brain, leading to disease progression or recurrence, either locally or distant from the primary tumor, appearing in the brain stem, cerebellum, and spinal cord **(Wainwright et al., 2012)**. GBM was initially thought to originate exclusively from glial cells, however, experimental evidence has shown that this tumor may also derive from different cell types with properties of neuronal stem cells that are at multiple stages of differentiation from stem cell to neuron to glia, with phenotypic variations determined, in large part, by molecular alterations in signaling pathways rather than by differences in cell type of origin **(Phillips et al., 2006)**. This subpopulation of highly tumorigenic cells, glioblastoma stem cells (GSCs) appears to be responsible for the recurrences of glioblastoma, presenting the capacity to self-renew, differentiate into multiple lineages, and for tumorigenesis. Unlike the bulk of the rapidly dividing tumor cells, GSCs are thought to

be relatively quiescent, rendering them resistant to conventional chemo- and radiotherapy **(Chen et al., 2012)**.

GBMs can be classified into primary or secondary: tumors that occur *de novo*, without therefore evidence of a malignant precursor are defined primary while those that develop from diffuse or anaplastic astrocytomas are defined secondary. Most GBMs are primary (~90%) **(Ohgaki et al., 2013)** and patients with this cancer tend to be older (~55 years old) than those with secondary GBM (~40 years old), who are also associated with a better prognosis and increased overall survival time compared with primary GBM. Although largely indistinguishable based upon histopathology, primary and secondary GBMs evolve from different genetic precursors and harbor distinct genetic alterations **(Watanabe et al., 1996)**.

Failure of conventional treatments combined with its poor prognosis highlights the need for novel approaches for GBM that are targeted at residual tumor cells in order to prevent recurrence.

Glioblastoma treatment strategies

Conventionally, therapeutic strategies aim at increasing patient life expectancy. The lethality of the GBM is mainly attributed to the limits of tumor treatment due to high average age of onset, tumor location, and poor current understandings of the tumor pathophysiology **(Louis et al., 2007)**.

The golden standard intervention for patients includes maximal surgical resection with radiotherapy (RT) to the resection cavity and concomitant adjuvant chemotherapy **(Fig.1).** The most frequently used chemo-drug is Temozolomide (TMZ) as it has been shown to pass the blood-brain barrier (BBB) and it is delivered orally **(Harder et al., 2018)**. The combination of radiotherapy with TMZ is the most efficacious adjuvant therapy to prolong survival after primary resection.

The goal of surgery is to achieve total tumor resection without compromising neurological functions. In fact, the organ in which this tumor grows, the brain, greatly limits the area of surgical removal, since each brain area corresponds to a vital function that prevents extensive tissue resection. In fact, despite improvements in imaging techniques such as magnetic resonance imaging (MRI), awake craniotomy, stereotactic

guidance, cortical mapping, diffusion tensor imaging and fluorescent-guided resection that have allowed surgeons to more accurately delineate the margins of the tumor and to perform a safer resection, the total removal of the tumor is almost impossible, given the anatomical structure that it invades **(Anton et al., 2012)**.

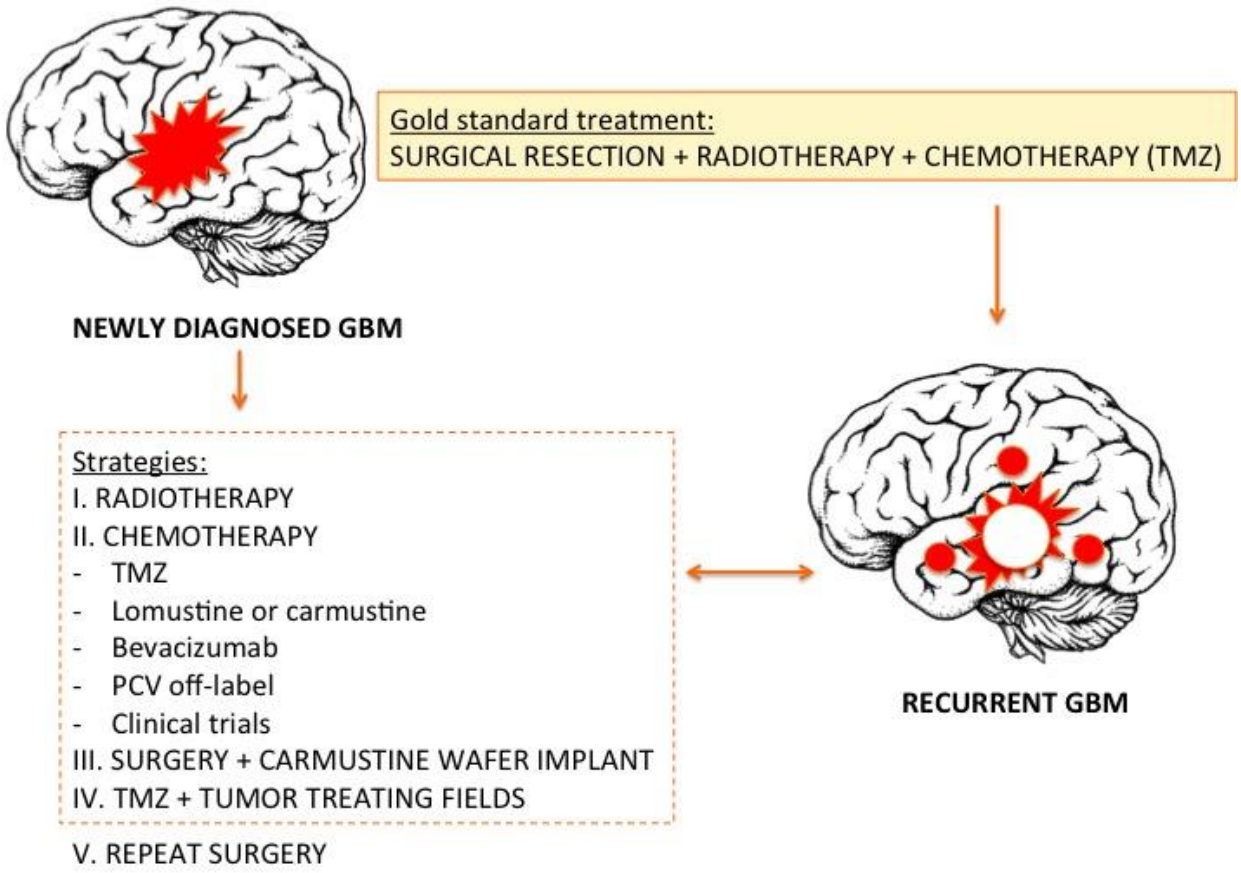

Figure 1. Schematic representation of GBM treatment strategies (modified from Bastiancich et al., 2016).

The current standard radiotherapy approach for glioblastoma patients is the most effective and is focal, fractionated external beam radiation therapy (EBRT) to cavity formed by the surgical closure of the tumor and to a 2 cm margin of the surrounding brain tissue. In this way ionizing radiation induces single-strand and double-strand

breaks in the DNA of proliferating cells **(Clarke et al., 2010)**. Since the life expectancy given by the use of radiotherapy alone is not very long, other adjuvant approaches have been investigated, including chemotherapy. The inclusion of TMZ in the treatment of glioblastoma has significantly increased the life expectancy of patients. In fact, clinical trials have shown that surgical removal of the tumor alone leads to a patient survival of approximately 6 months, while combining surgery with radiotherapy can extend this period to 12.1 months. Finally, by adding chemotherapy with TMZ to these two approaches, life expectancy can be increased to 14.6 months **(Stupp et al., 2005)**. However, despite advances with adjuvant therapies, surgical removal remains the most important step in the treatment of GBM, allowing for a histologic confirmation of the diagnosis as well as cytoreduction.

The use of chemotherapeutic agents is a necessary treatment against cancer cells left in the brain after surgical removal of the tumor, to avoid recurrence. The chemo-drug TMZ performs its therapeutic task by adding a methyl group to the purine bases of DNA. This addition leads to damage to DNA ,which therefore triggers a signal cascade ultimately inducing apoptosis of cancer cells **(Day et al., 2012)**. The main target of TMZ is O6-methylguanine, which, once received the methyl group, can trigger the cell death process. The obstacle to this process is the presence in the cells of O6-methylguanine methyltransferase (MGMT), a DNA repair protein capable of removing the added methyl group. This enzyme, repairing DNA damage caused by TMZ, confers resistance to cancer cells, protecting them from chemotherapeutic alkylating agents. A mechanism to counteract the chemoresistance given by MGMT activity is gene silencing. In fact, by methylating the regions of the gene promoter, the protein is prevented from removing the methyl groups added to the O6 position of the guanine **(Villalva et al., 2012)**. Thus, patients with an unmethylated MGMT are much less responsive to TMZ, whereas MGMT methylation confers sensitivity to TMZ in patients with GBM, making the methylation status of the promoter region of the MGMT gene one of the main mechanisms on which to act to alter the sensitivity/resistance of tumor cells to TMZ **(Drablos et al., 2004)**.

However, despite TMZ being able to pass the BBB, the percentage of drug that reaches the target site is still very low. Furthermore, two to three weeks usually elapse between

the surgical removal of the tumor mass and the start of adjuvant therapies. During this period, the cancer cells left in the brain give rise to a relapse. For these reasons GLIADEL, a delivery device based on a rigid matrix, has been designed to locally treat GBM on its site with Carmustine. The advantage of using GLIADEL is that it is positioned inside the brain cavity generated during surgical removal of the tumor, whereby Carmustine is released directly into the brain, without having to pass the BBB. Similar to TMZ, Carmustine is a DNA alkylating agent. These biodegradable wafers impregnated with chemo-drug come in contact with the edges of the tumor, allowing the controlled release of Carmustine for several weeks. In this way the drug is released into the surrounding brain tissue immediately after the surgical operation and can perform its alkylating action for a long time **(Anton et al., 2012)**.

Although clinical trials have shown how the use of Carmustine in combination with RT and TMZ has modestly increased the life expectancy of patients, the complications associated with their use, such as infections, need for removal, swelling and impairment of wound healing, prevent the daily use of these wafers in most hospitals **(Hart et al.,2008; McGirt et al., 2009)**.

Characteristics of GBM and obstacles for effective treatment

Indeed GBM presents some hard features that characterize its invasiveness and make it so hard to find therapy to prevent its recurrence and increase patients' life expectancy **(Fig.2)**. First, its anatomic site: in fact, the GBM, originating and expanding within the central nervous system (CNS), is separated from the blood by the blood-brain barrier, a vasculature composed of highly specialized endothelial cells (**Bastiancich et al., 2016**). This barrier performs very important functions of nourishment to the CNS through a selective uptake of small molecules and protection by actively extruding xenobiotics from the blood. This unique dynamic cellular complex is characterized by the fact that the endothelial cells fit tightly together giving origin to a continuous endothelium which is not fenestrated, and which exhibits a relatively low endocytic activity. However, the BBB creates an obstacle to the effective delivery of drugs necessary for treating pathological conditions of the CNS from neurological diseases to cancer. It is indeed difficult for drug to reach the specific target inside the brain.

In addition, malignant glioblastomas are heterogeneous tumors in both appearance and gene expression, exhibiting the greatest range of genetic abnormalities. In fact, high dimensional genomic profiling has made it possible to classify GBMs into four subtypes, distinguishing them for genetic alterations and molecular profiles: classic, mesenchymal, proneural and neural **(Beroukhim et al., 2007)**. Gene heterogenicity and the different expression patterns of this tumor do not allow for a single effective therapy for all glioblastoma subtypes.

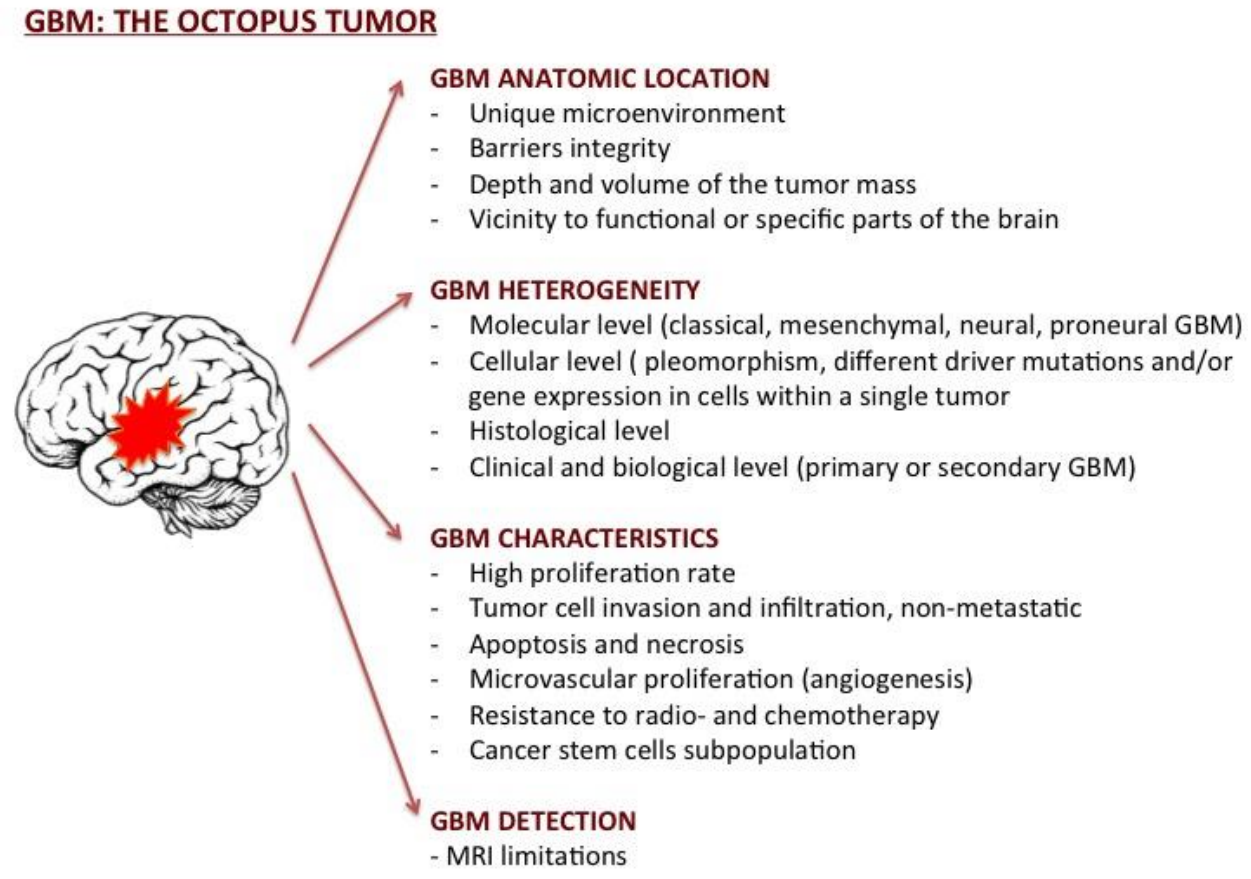

Figure 2. Schematic representation of GBM characteristics (modified from Bastiancich et al., 2016)

Another feature of glioblastoma is its aggressive and invasive nature. Indeed these tumors show high proliferation rate, which leads to the formation of a tumor mass without clear margins, therefore not amenable to a complete resection, which is the main cause for remissions. Moreover GBM shows a strong resistance to radio- and chemotherapy that determine a limited therapeutic response. In fact, cancer stem cells (CSCs) from these tumors commonly express drug-resistance proteins, such as Multidrug Resistance 1 (MDR1) transporters, which might render them resistant to chemotherapy and apoptosis induction **(Chaudhary et al., 1991)**. MDR1 protein is expressed in CSCs at higher levels than differentiated cancer cells, favoring undifferentiated cancer cells resistance to chemotherapy, including the treatment with TMZ and other alkylating agents **(Liu et al., 2005)**. This chemoresistance explain the high frequency of tumor recurrence with existing cancer therapies. In fact, despite the ability of chemotherapy to eliminate the most differentiated cancer cells, the persistence of CSCs prevents the reduction of the tumor, allowing its growth and invasion of the surrounding brain tissue.

The other main problem of glioblastoma management is related to the lack of effective diagnostic strategies. Currently, the main diagnostic methods for the detection of gliomas rely on neurological tests and neuroimaging methods, performed when the disease is already at an advanced stage **(Posti et al., 2015)**. Late diagnosis of GBM is mainly caused by the slow dissemination process typical of brain tumors, which allows structures to gradually adapt to both compression and deformation caused by the tumor mass. For this reason, even in the case of pronounced morphological signs of tumor penetration into brain tissue, clinical manifestations may be completely absent **(Sizoo et al., 2010)**.

All these characteristics inevitably lead to the appearance of a recurrence and make glioblastoma a tumor practically impossible to defeat.

Strategies to cross BBB

BBB is mainly responsible for rigorously controlling the exchanges between the two compartments allowing only certain molecules or ions to pass through by diffusion or occasionally by more specialized processes of facilitated diffusion, passive transport, or

active transport (**Bellettato et al., 2018**). Being the tightest endothelium in the body, the BBB also represents the main impediment to drug delivery to the brain. Research has therefore focused on understanding the molecular and physiological mechanisms that govern the transport of compounds through the BBB in order to solve the problem of drug delivery into the brain. Generally, only lipid soluble (lipophilic) molecules with a low molecular weight (under 600 Da) and positive charge can cross the BBB (**Bellettato et al., 2018**). Other molecules require cell endogenous transport systems, such as carrier-mediated transport, receptor-mediated transport, or absorptive-mediated transport. Commonly, there are five basic mechanisms by which solute molecules move across membranes **(Fig.3A)**.

The first is simple (or passive) diffusion. This is a spontaneous process guided by the concentration gradient and the correlation between the increased solubility of the lipid and the rate of penetration into the brain **(Tosi et al., 2013)**. The second transport mechanism takes place via solute carriers (SLC). These carriers are a family of membrane transport proteins that facilitate the bidirectional movement of solutes across the cell membrane. SLC transport does not require ATP since it is driven either by electrochemical gradients (i.e. Na+ or H+ gradient) or by concentration gradients established by the solutes that are being transported **(Sanchez-Covarrubias et al., 2014)**. SLC are therefore classified as either facilitated transporters or secondary active transporters. Among the major nutrients that use this type of transport are glucose, amino acids, nucleosides, organic anions and cations **(Begley et al., 2008)**. The third transport mechanism is carrier-mediated efflux. This includes ATP-binding cassette (ABC) transporters that use ATP hydrolysis to push molecules across the membrane and to force the efflux of solutes against the concentration gradient. ABC transporters have a broad affinity with various categories of solutes including large lipid-soluble molecules containing hydrogen and oxygen atoms in their structures **(Begley, 2004)**. Fourth, there is receptor-mediated transcytosis, a mechanism that uses the vesicular transport system of endothelial cells to transport substrates across the barrier. This receptor-mediated transcytosis (RMT) is induced by the binding of large molecules such as peptides or proteins to their highly expressed receptors on the membrane of endothelial cells. (e.g. iron, insulin and leptin) **(Scarpa et al., 2015)**. The last transport

mechanism is represented by the diapedesis of mononuclear leukocytes, which allows the crossing of the BBB by migrating directly through the cytoplasm of endothelial cells without the disruption of tight junctions. Once they enter the brain, they become microglia, the CNS immunocompetent cells **(Muldoon et al., 2013)**.

Despite these numerous transport mechanisms, it has been estimated that more than 90% of all small-molecule drugs and nearly 100% of all larger therapeutics are not able to overcome the BBB **(Pardridge, 2005)**.

In the past years many attempts have been made to use non-invasive techniques to cross the BBB to deliver therapeutic products to the CNS. This approach mainly consists in the development of pharmacological strategies capable of modifying drugs to facilitate transport across the BBB.

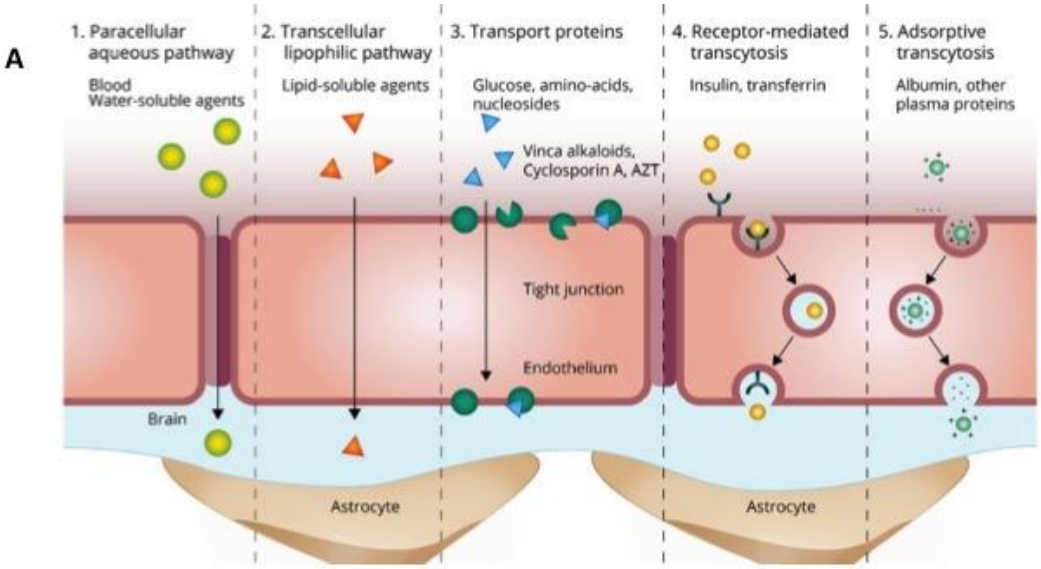

Cuggino et al., 2019. *Crossing biological barriers with nanogels to improve drug delivery performance.*

Brem H et al., 2017. *Developing therapies for brain tumor: The impact of the Johns Hopkins hunterian neurosurgical research laboratory.*

Figure 3. Strategies to cross BBB. Nano-carriers able to actively cross the BBB (A) (adapted from Cuggino et al., 2019); Intracranial delivery of drugs (B) (adapted from Brem et al., 2017).

Among the various non-invasive techniques developed such as the inhibition of efflux transporters to prevent drug delivery, trojan horse approach, chimeric peptides, modifications to increase the lipid solubility of the drug, monoclonal antibodies fusion proteins and gene therapy, the use of nano-carriers as transport systems emerges, which involves a chemical modification of a small-molecule drug to allow it to use the endogenous transport system, mimicking the structure of the related endogenous molecule (e.g. amino acids, monosaccharides, nucleosides, vitamins, hormones, etc.).

However, despite the different strategies studied to cross the BBB, to date the most effective treatment can only occur after surgery and local placement of scaffolds of nanofibers containing entrapped Carmustine, a lipophilic chemotherapeutic drug that

treats brain tumors by alkylating DNA and inhibiting the further synthesis of DNA, RNA, and protein **(Fig.3B)**.

In 1996, the Carmustine-enriched implant GLIADEL was approved by the US Food and Drug Administration (FDA) as an effective local treatment for recurrent malignant glioma **(Brem et al. 1995)**. It is the first and currently the only available local drug delivery treatment of brain tumors with FDA approval. GLIADEL wafers are composed of Carmustine distributed homogeneously and are implanted along the walls of the resulting cavity following surgical resection of a tumor. As the wafers degrade, they deliver Carmustine to the surrounding cells over the course of about 3 weeks **(Attenello et al., 2008)**.

To date, Carmustine is a fairly obsolete chemotherapeutic drug and therefore the need to develop new drug delivery strategies to overcome the BBB for the treatment of brain tumors such as glioblastoma is evident.

Smart materials: thermogels

In recent years, a huge number of studies have been carried out for the development and use of so-called "smart materials" as drug delivery systems. These materials can change their properties when an external stimulus is applied and according to their characteristics they can be loaded with different drugs. This therefore allows the release of active molecules at the target site at optimal concentrations, without causing pharmacological toxicity to the rest of the organism. Different materials such as liposomes, polymeric systems, nanomaterials and hydrogels can respond to different stimuli such as pH, temperature and light and these are all attractive systems to employ for achieving controlled release applications. In this context of progress, the use of hydrogel as a new system of drug administration emerges.

Hydrogels are three-dimensional (3D) polymeric and hydrophilic networks able to imbibe large amounts of water or biological fluid without the dissolution of the polymer due to their hydrophilic but cross-linked structure. Hydrogels exhibit a thermodynamic compatibility with water, which allows them to swell in aqueous media **(Peppas et al., 2000)**. Among the qualities of hydrogels emerges that of controlled release, thus also

allowing targeted drug delivery, being able to encapsulate macromolecules such as hydrophilic or hydrophobic drugs but also DNA and proteins **(Lin et al., 2006)**.

In fact, these gels are highly compatible with a range of drugs, which are soluble, insoluble, showing either low or high molecular weight; they are less invasive and can be used to obtain high drug concentrations at the desired site of action with reduced systemic side effects **(Aderibigbe, 2018)**. Moreover, this delivery system can be used for various applications such as oral, rectal, ocular, epidermal and subcutaneous.

A key point in the success of hydrogels development is the *in situ* gelation.

In fact, they are liquid when administered and undergo a sol-to-gel transition which can be achieved by UV polymerization, introducing non-reversible covalent bonds, or via self-assembly by either reversible interactions or non-reversible chemical reactions. The gelation can also be time-dependent or be triggered by specific stimulus (e.g. pH, temperature, light, etc.) **(Van Tomme et al., 2008)**.

Within these innovative gels, particular attention has been paid to thermogels. In fact, these gels are attractive candidates for targeted drug delivery because thermogel has reverse gelation properties, this means that the sample at low temperatures assumes the consistency of a viscous aqueous solution and the viscosity of which increases as the temperature (37°C).

The advantage is that these copolymers can be injected in a liquid form, if kept at 4°C until the time of administration and when it is exposed to body temperature, the solution becomes a solid gel that gradually releases the encapsulated drug.

Literature **(Karim et al., 2016)** shows these systems can be directly administered in the brain after a craniotomy via intracerebral implantation or intracerebroventricular injection. They can be administered intratumorally or in the surgical resection cavity. In some cases, the drug is directly loaded in the hydrogel matrix while some authors have incorporated anticancer-loaded nanomedicines into the hydrogels, in order to prolong the sustained release of the drug **(Fig.4)**. Even if the administration of hydrogels in the GBM resection cavity is very seldom described in the literature, this route of administration seems very promising due to its clinical relevance.

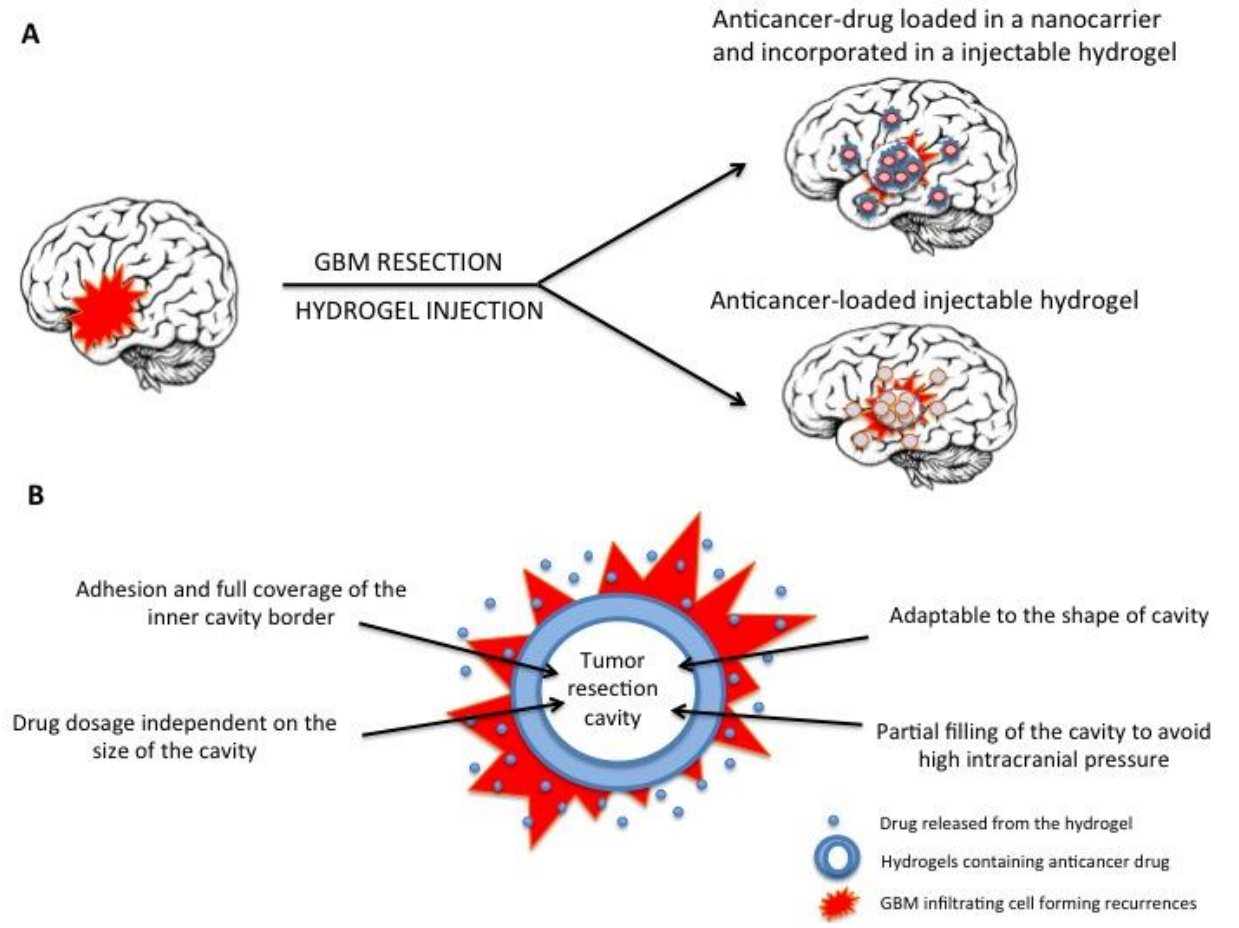

Figure 4. Schematic representation. The use of anticancer-loaded hydrogels for the treatment of GBM (A) and the clinical issues related to the development of injectable hydrogels for the treatment of GBM (B) (adapted from Bastiancich et al., 2016).

Materials and Methods

In vitro experiments

MTS assays

MTS assay is a sensitive colorimetric method for the quantification of viable cells in cell proliferation assay. The NAD(P)H-dependent dehydrogenase enzymes in metabolically active cells causes the reduction of MTS tetrazolium compound and generates the coloured formazan product that is soluble in the cell culture medium. Since only viable cells can convert the MTS tetrazolium compound into formazan, the yield of significant increase in color intensity, quantified by measuring the absorbance at 490-500 nm is directly correlated to the amount of viable cells.

To perform these assays we used *CellTiter 96® AQueous One Solution Cell Proliferation Assay (Promega)*. DBTRG and U87MG ($1x10^3$) cells were seeded in 96-well in their culture medium (U87MG: Eagle's Minimum Essential supplemented with 10% fetal bovine serum, 100 U/mL penicillin and 100 µg/mL streptomycin; DBTRG: Dulbecco's Modified Eagle's Medium supplemented with 10% fetal bovine serum, 100 U/mL penicillin and 100 µg/mL streptomycin) and incubated in 5% CO2 at 37°C over night. The next day, cells were treated in triplicate with increasing concentrations of Temozolomide (used in a range of 0-1500 µM). After 72h of treatment, 20 µl of *CellTiter 96® AQueous One Solution Reagent* were pipetted into each well of the 96-well assay plate containing the cells in 100 µl of culture medium.

The assay plate was incubated at 37°C for 2 hours in a humidified, 5% CO_2 atmosphere. The absorbance was recorded at 490 nm using the 96-well plate reader SpectraMax (VersaMax™ Microplate Reader, Molecular Devices).

Each experiment was set in triplicate and results are given as mean ± SEM of absorbance. The statistical analysis and calculation of IC50 were performed using the *GraphPad Prism software*.

Biocompatibility test of the thermogel: toxicity and release of TMZ

The aim of our project is to use a proprietary thermogel containing TMZ for the treatment of glioblastoma. Our aim is to use this gel placing it directly onto the brain tissue. Therefore, we carried out preliminary experiments to evaluate its toxicity and biocompatibility. To this end, we first analyzed the effect on cell adhesion, cell morphology, cell viability and cell proliferation in a U87MG cell culture. For a complete characterization, we compared the effect of the empty gel and the effect of the gel loaded with TMZ. The latter experiment is mandatory to verify the chemotherapeutic release from the gel, measuring its cytotoxic effect on U87MG cells.

U87MG cells ($2x10^5$) were plated in 6-wells in their culture medium. After 24h, cells were treated either with fresh medium (control), with a correspondent volume (20 µl) of empty or TMZ loaded gelin its liquid form. After 72h of treatments, the medium was removed, cells were washed in PBS and trypsinized and prepared for cell count. 200 µl of solution containing the cells was added to 9.8 ml of *Isoton II diluents solution*, a filtered phosphate-buffered saline solution compatible with human cells, and three counts were performed for each well, using the *Z2 particle count and size analyzer*(Beckman Coulter). Each experiment was set up in triplicate and results are given as mean ± SEM. The statistical analysis was performed using the *GraphPad Prism software*.

In parallel, a similar experiment was set up to verify cell morphology. Here, 72h after the treatments cells were analyzed under an optical microscope (OLYMPUS CKX41).

Luciferase assay

Luciferase assays were performed to verify the bioluminescence of U87MG-Red-FLuc human glioblastoma cells in order to use them as *in vivo* model to monitor tumor growth. The U87MG-Red-FLuc *Bioware® Brite Cell Line* is a light-producing cell line derived from U87MG human glioblastoma. The cells have been stably transduced with the red-shifted firefly luciferase gene of *Luciola Italica* (Red-FLuc), to provide a brighter, red-shifted signal.

Bioluminescence arises when luciferase, a monomeric 61kDa protein, catalyzes firefly luciferin oxidation using ATP•Mg2+ as a co-substrate to form oxyluciferin, ATP and CO_2. To carry out this essay we used the *Luciferase Assay System* (Promega). U87MG and

U87MG-Red-FLuc cells ($3x10^5$) were plated in triplicate in 6-well in their culture medium. After 24h, we added 4 volumes of water to 1 volume of 5X lysis buffer and equilibrated 1X lysis buffer to room temperature before use, as from maker's notes. We carefully removed the growth medium from cells to be assayed, rinsed cells with PBS, being careful to not dislodge attached cells and removing as much of the PBS rinse as possible. Then, we added 400 µl of 1X lysis buffer and rocked culture dishes several times to ensure complete coverage of the cells with lysis buffer. We scraped attached cells from the dish and transferred cells to a microcentrifuge tube on ice. We vortexed the tube 10-15 seconds, then centrifuged at 12.000 x g for 15 second at room temperature. Then we proceeded with the luminometer analysis. We dispensed 100 µl of *Luciferase Assay Reagent* into microcentrifuge tubes and we added 20 µl of cell lysate by pipetting 2-3 times. We programmed the luminometer to perform a 2-second measurement delay followed by a 10-second measurement read for luciferase activity.
Each reading of the sample was performed in triplicate and each experiment was set up in triplicate. Results are given as mean ± SEM. The statistical analysis was performed using the *GraphPad Prism software*.

Preliminary *in vivo* experiments

Biocompatibility test of the thermogel: brain tissue toxicity

Preliminary *in vivo* experiments were set up to verify the biocompatibility of the thermogel in the brain tissue using the same animal model chosen for the glioblastoma treatment experiment to minimize variability. The experiment involves brain microsurgery, a delicate procedure performed applying all the possible requirements of refinement (according to 3R guidelines).
To perform intracranial injections, we took advantage of the stereotaxic table equipped with a 3-axe system micromanipulator to aim at selected target regions and a holder to accommodate a Hamilton syringe. The stereotaxic table can accommodate a nosecone for anesthetizing the animal and body temperature and breath rate can be monitored. The system of coordinates used for these experiment were derived from the Paxinos Atlas of mouse brain. The tri-dimensional system is applied internationally to

unequivocally describe a point or an area of the brain based on a longitudinal and latitudinal positioning (in millimeters) originating from bregma, the point on the skull that become visible once the skin is removed, identified by the interception of coronal and median sulci. Depth can be added to intercept different subcortical areas. To check for the correspondent areas, a series of detailed two-dimensional reference images of brain slices taken every millimeter for the entire volume of the representative brain is available.

Animals were anesthetized using an induction chamber, to allow mixing of the isoflurane and oxygen, until absence of toe-pinch reflex was verified. Once the mouse was fully sedated, we carefully removed the mouse from the induction chamber, placing it on the stereotaxic apparatus over the heating pad, set at 37°C and anesthesia was maintained for the whole duration of the surgery [setting 1.5% (wt/vol) isoflurane (range 0.9-1.8%) in 100% oxygen (0.5 l/min)]. Animals were adjusted on the stereotaxic apparatus and fixed to the incisors bar, inserting the upper central incisors into the hole and the ear-bars into the each acoustic meatus, repositioning the nosecone to avoid aesthetic leaking.

To prevent drying and cataract formation due to the anesthetic procedure, we covered the eyes with *Puralube* ophthalmic ointment. Positioning of the mouse's body and head is fundamental to proceed with the surgery as an erroneous positioning might imply a mistake in the referenced positioning of the coordinates. Moreover a hindered movement could seriously hurt the animal head neck and trunk. In fact, excessive head elevation can impair breathing. It was important to verify that the restraining applied was sufficient to prevent any movement, while preserving moderate intraocular pressure.

We next applied *Betadine* solution on the scalp and then proceeded with incision. We hold the scalpel handle attached to a sterile blade and started the incision ~12–15 mm long at the midline, ~3 mm posterior to the eyes. To excise the epidermis from the scalp, we used forceps to pull the skin taut at the top left side of the incision, using a pair of push scissors to excise the skin over the left hemisphere of the skull and we finished cleaning any remnants from the skull using sterile cotton-tipped applicators moistened with sterile saline.

At this point, we proceeded with the craniotomy. We used a forceps with the tips closed together to tease away the lateral muscles and we proceeded using a dental drill to

lightly etch the circumference of the craniotomy. The most important thing is avoiding drilling the same area for more than 2 seconds to prevent overheating due to friction. Doing so, we thinned down the skull around the outside perimeter of the craniotomy, irrigating with sterile saline intermittently to prevent overheating of the superficial brain mater. Once the surrounding skull began to separate, we submerged the skull in sterile saline and gently removed the bone flap using tweezers exposing the brain surface.

For this experiment, animals were divided into two different groups: sham (animals with craniotomy but without gel treatment) and mice that underwent craniotomy and gel treatment. For the latter group thermogel was gently laid on top of the exposed brain tissue within the cranial window.

At this point a *dura mater* substitute, *Duraform, was used* to cover the missing part of the scull and the skin was sutured using tissue glue (Vetbond). Animals were then replaced into their cages, under a warm light and monitored until awake.

Setting the *in vivo* model of glioblastoma

Optimization of model setting was performed to obtain reliable result of treatment of brain tumor and recurrences. We tested two different human glioblastoma cell lines, two different cell concentrations and two different inoculation coordinates inside the brain **(Fig.5).**

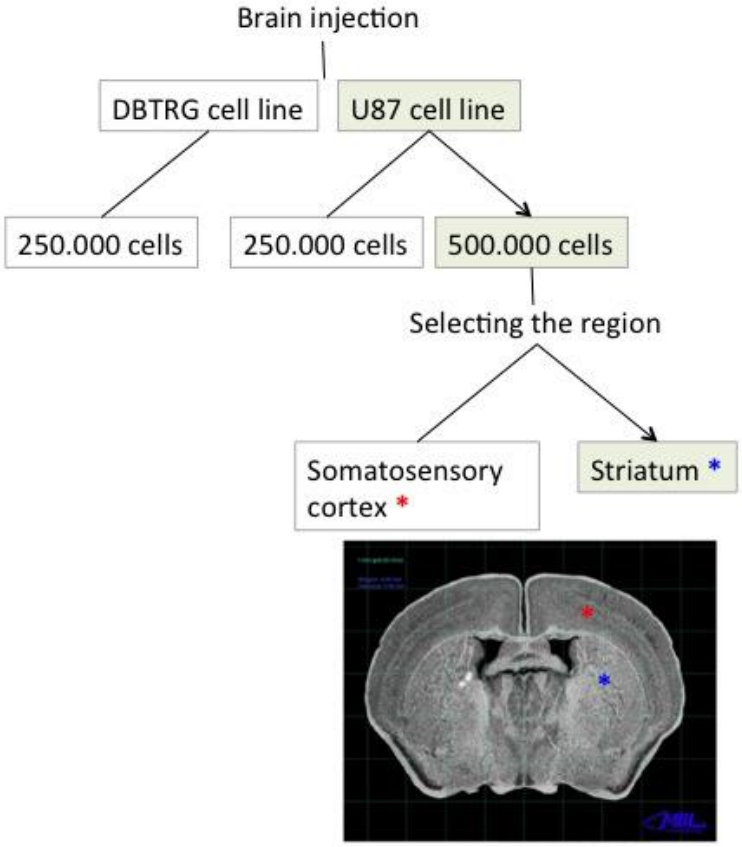

Figure 5. Schematic representation of set up of an orthotopic model of GBM in mouse

Cell model identification and Inoculum preparation

DBTRG and U87MG human glioblastoma cell lines were tested in our laboratory to verify growth rate capability of each line in the brain tissue: cells in their culture medium were washed in PBS, trypsinized and counted using the Beckman Coulter Counter Z2, as previously described. Cells were then transferred into a sterile tube, centrifuged at 1200 rpm for 5 min, re-suspended and washed in PBS 1X, then re-suspended in PBS 1X to a concentration of $1x10^5$ cells per µl and kept on ice until the time of intracranial inoculation.

Intracranial injection

Cells were inoculated in an area corresponding to the somatosensory cortex of 5-6 weeks nude female mice. As described, stereotaxic apparatus was used to fix anesthetized mice, monitored and ventilated. After defining Bregma (Y=0 and X=0), the point of injection was identified as +0.5 mm lateral (x); 1.75 mm antero-posterior (y): a burr hole was performed in the cleaned exposed skull of each animal gently twisting a siring needle by hand until the skull bone is consumed and the aperture is visible. Just prior to injection, we freshly mixed by pipetting the cell suspension and we loaded a Hamilton syringe with $5x10^5$ tumor cells in 5 µl of PBS 1X. We gently lowered the Hamilton needle into the hole to reach brain tissue. From surface (0.0 mm) the needle tip reached 0.9 mm depth into the brain to reach deep cortical structure. Cells were slowly hand-injected at 1 µl/min rate. The syringe was left in place for additional 5 min to avoid cell leaking. Skull skin was sutured using *Vetbond* tissue glue **(Fig.6)**.

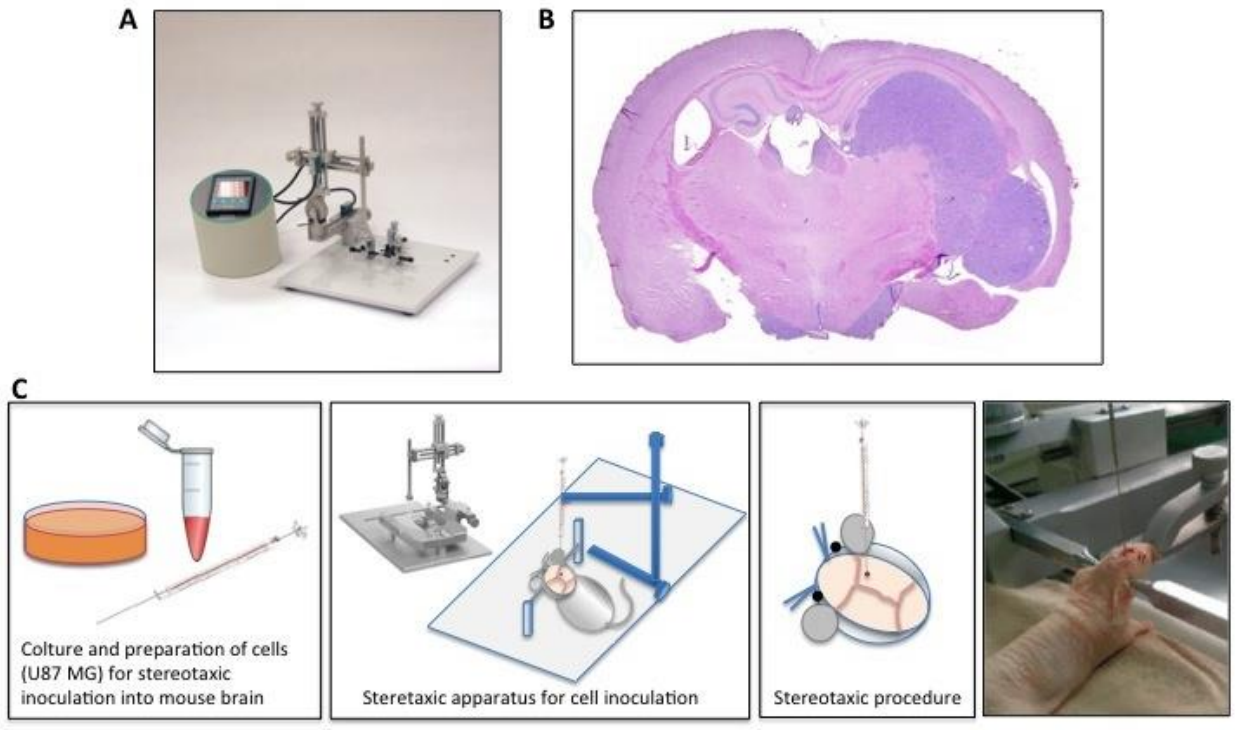

Figure 6. Schematic representation of mouse orthotopic model of human glioblastoma. The digital mouse stereotaxic instrument, available at Siena mouse facility, for intracranial injection of GBM cells (A). The histologic aspect of an orthotopic glioblastoma at 21 days post–inoculation. Colored with hematoxilin–eosin (B). Scheme of the stereotaxic procedure for intracranial cell inoculation (C).

After the end of the surgery, mice were monitored for recovery until completely awake. Remaining cells from each injection pool were re-plated onto new dishes to observe vitality and possible contamination during surgery.

This protocol was applied for testing the growth rate of two different concentrations of U87MG cells: $2.5x10^5$ and $5x10^5$ and subsequently for discriminating the feasibility of the setting using two different inoculation coordinates: the somatosensory cortex [(+0.5 mm lateral (x); 1.75 mm antero-posterior (y) more superficial (0.90 mm from the surface deep), and the striatum (1.90 mm from the surface deep)].

Tumor mass resection

To study of the effect of loaded thermogel on tumor relapse, we created a model of tumor resection. This is an extremely delicate surgical intervention. For this reason, in accordance with our approved protocol we decided to use deep anesthesia [intraperitoneal injection of Zoletil (10-40mg/kg) + xilazina (0.4-4 mg/kg)].

U87MG human glioblastoma cells were inoculated into the striatum of immunodeficient nude mice accordingly to the protocol described above. Seven days after the intracranial seeding, an incision was made in the midline along the previous surgical scar and a microsurgery was performed to create a cranial window in the animal skull in correspondence to the previous injection site **(Fig.7A-B)**. A biopsy punch with an incision tip of 3 mm depth and 2 mm wide diameter (World precision instruments) was used to produce a tissue extraction **(Fig.7C)** generating a small hole (circa 10 μ^3) in the brain in correspondence of the tumor mass. Liquid thermogel kept on ice (circa 5 microliters) was laid to fill the empty hole using an automatic micropipette **(Fig.7D)**. Finally, the open part of the skull was protected with *Duraform* and the flaps of skin attached as described above **(Fig.7E-F)**.

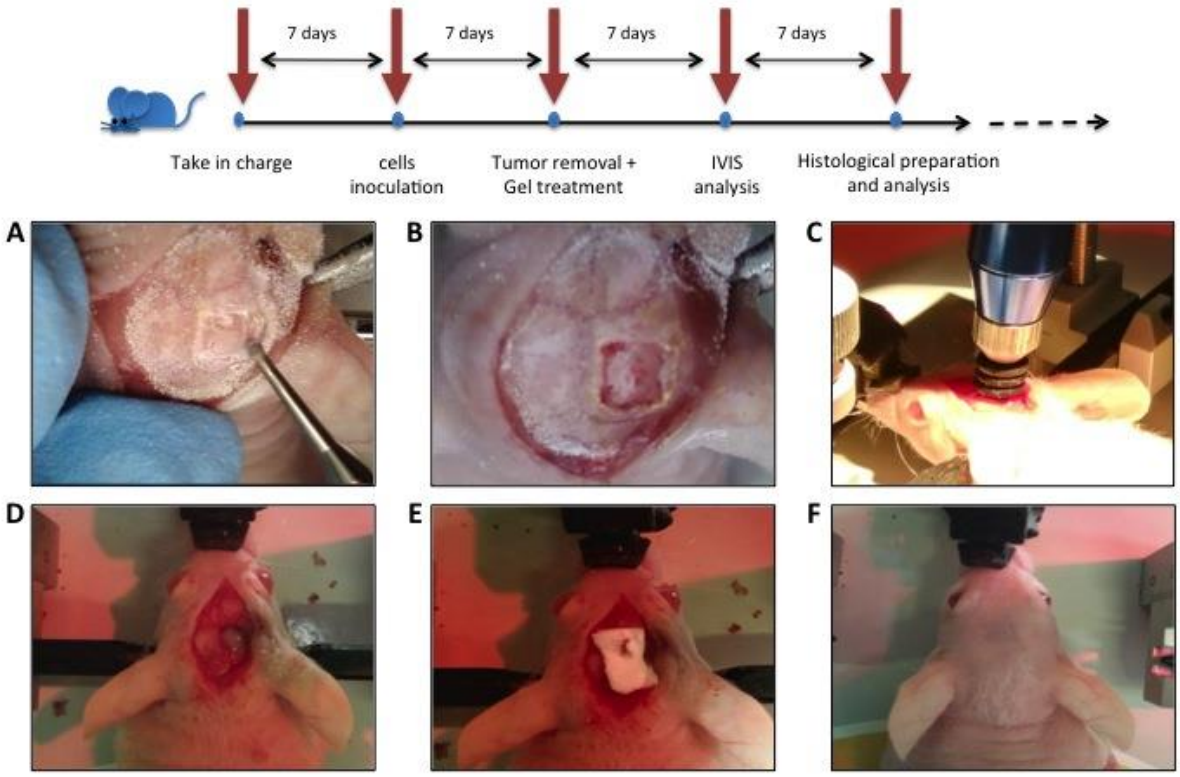

Figure 7. Craniotomy and tumor resection procedure. Craniotomy (A), Cranial window (B), Punch resection (C), Thermogel insertion (D), Duraform *Dura* replacement (E), Suturing after complete procedure (F).

For this experiments, mice in the control group were treated with the empty gel, while treatment group received thermogel loaded with TMZ 19.3 mM (3.744 mg/mL).

Mice were monitored until awake, controlling body temperature and breathing. Afterwards, to register animal general conditions, mice were weighed every four days recording any sign of discomfort such as weight loss, postural or behavioral motor changes. After 14 days of treatment, animal were euthanized accordingly to approved protocol.

Paraffin waxing and inclusion of brains

After sacrifice, brains were immediately excised, washed in PBS 1X, transferred in 5 ml of 10% paraformaldehyde for 21 day at 4°C. After 21 days of fixation, segments of the brain in correspondence with the affected areas were held into special paraffin embedding cassettes and washed to remove formalin from the tissue: absolute ethanol for 1 hour, 70% ethanol for 30 minutes, 50% ethanol for 30 minutes and water for 3-4 hours. At this point, we used an automatic paraffiner, a tissue processor (LEICA ASP200S), with the following program: 70% ethanol for 1 hour, 95% ethanol (95% ethanol/5% methanol) for 1 hour, first absolute ethanol for 1 hour, second absolute ethanol for 30 minutes, third absolute ethanol for 30 minutes, fourth absolute ethanol for 2 hour, first clearing agent (Xylene) for 1 hour, second first clearing agent (Xylene) for 1 hour, first wax (Paraplast X-tra) at 58°C for 1 hour, second wax (Paraplast X-tra) at 58°C 1 hour.

To finalize embedding, we used an automatic wax dispenser with liquid wax (70°C paraffin). The specimen was molded in shaped cassettes to facilitate the use at the microtome: more specifically, using warm forceps, we transferred brain into mold, placing cut side down, as it was placed in the cassette. We transferred mold to cold plate, and gently pressed tissue flat. Paraffin will solidify in a thin layer, which holds the tissue in position. When the tissue was in the desired orientation, we added the labeled tissue cassette on top of the mold and pressed firmly. We added hot paraffin to the mold from the paraffin dispenser to be sure there was enough paraffin to cover the face of the plastic cassette. Over a cold plate at 4°C, paraffin was left to solidify in 30 minutes. When the wax was completely cooled and hardened (30 minutes) the paraffin block could be easily popped out of the mold; the wax blocks should not stick. The tissue and paraffin attached to the cassette has formed a block, which is ready for sectioning.

Sectioning tissue

Tissues were sectioned using a microtome (Leica RM2125 RTS) equipped with a water-bath with fresh deionized water at 35-37ºC that receives the slices once cut. Before starting collecting the relevant slices, we placed the specimen block controlling for the right orientation. For our purposes, 7 µm thick sections were collected approximately every 50 µm (1 slice over 7). The selected slice was let flowing into the warm bath and

collected on a clean superfrost glass slides to be processed for staining. Slides with paraffin sections were left on the warming block in a 37°C incubator over night.

Hematoxylin and Eosin staining

Once the slides containing the brain sections of our interest were obtained, we proceeded with the staining of the histological preparations with hematoxylin and eosin. Hematoxylin is a vegetable dye, extracted from the wood of a legume, the *Haematoxylum campechianum,* and dyes violet blue all negatively charged cellular components, such as nucleic acids, membrane proteins and cell membranes. Eosin instead dyes pinkish red all positively charged cell components, such as many cellular proteins, mitochondrial proteins, collagen fibers and extracellular substances.

We positioned the slides in special staining cassettes and performed a series of washes to remove the paraffin from the tissues: 3 one-minute washes with Xilene I, 3 one-minute washes with Xilene II, 3 one-minute washes with EtOH Ass, 3 one-minute washes with EtOH 95%, 2 one-minute washes with EtOH 80%, 2 one-minute washes with EtOH 70%, 2 one-minute washes with EtOH 50%, and 2 minutes washes with water. Then we incubated the slides 20 minutes with Hematoxylin, covering the pan with aluminium foil. We then washed the slides with running tap water for 10 minutes and incubated with Eosin for 40 seconds. Finally we washed with running tap water for 10 minutes. We used a fine tip vacuum pumped to dry the empty parts of the glass leaving a few droplets of water on the tissues. A drop of Faramount, Aqueous Mounting Medium (Dako), close to the brain sections was used to finalizing the coverslip application and then the slides in an oven at 37 ° C for an hour to dry them.

Histological analysis was performed under an optical microscope (OLYMPUS CKX41).

Measurement of the tumor area

The optical microscope was equipped with an image capturing system and an processing software (NIS 2.3) that allowed offline analysis of the results.

All the sequential images of the slides were recorded, identifying the beginning (most frontal appearance) and the end (most rostral appearance) of the tumor mass in the brain tissue. The NIS 2.3 software allowed us to measure the perimeter of the tumor in

each section, rendering the area in pixels. The total area for each tumor was calculated by adding the area of the tumor mass present in each individual section.
Results are given as mean ± SEM. The statistical analysis was performed using the *GraphPad Prism software*.

IVIS imager live analysis

In parallel to the histological analysis of the brains, experiments with U87MG-Red-FLuc cells were set up in order to carry out bioluminescence analysis to monitor tumor growth without sacrificing the animals. We used the IVIS system, a live imaging luciferase-based instrument (MS Lumina X5, Perkin Elmer) **(Fig.8)** for the study of the treatment of tumor recurrence as IVIS also has the advantages to check for small quantity of tumor cells, that will be quite difficult to detect by histology.

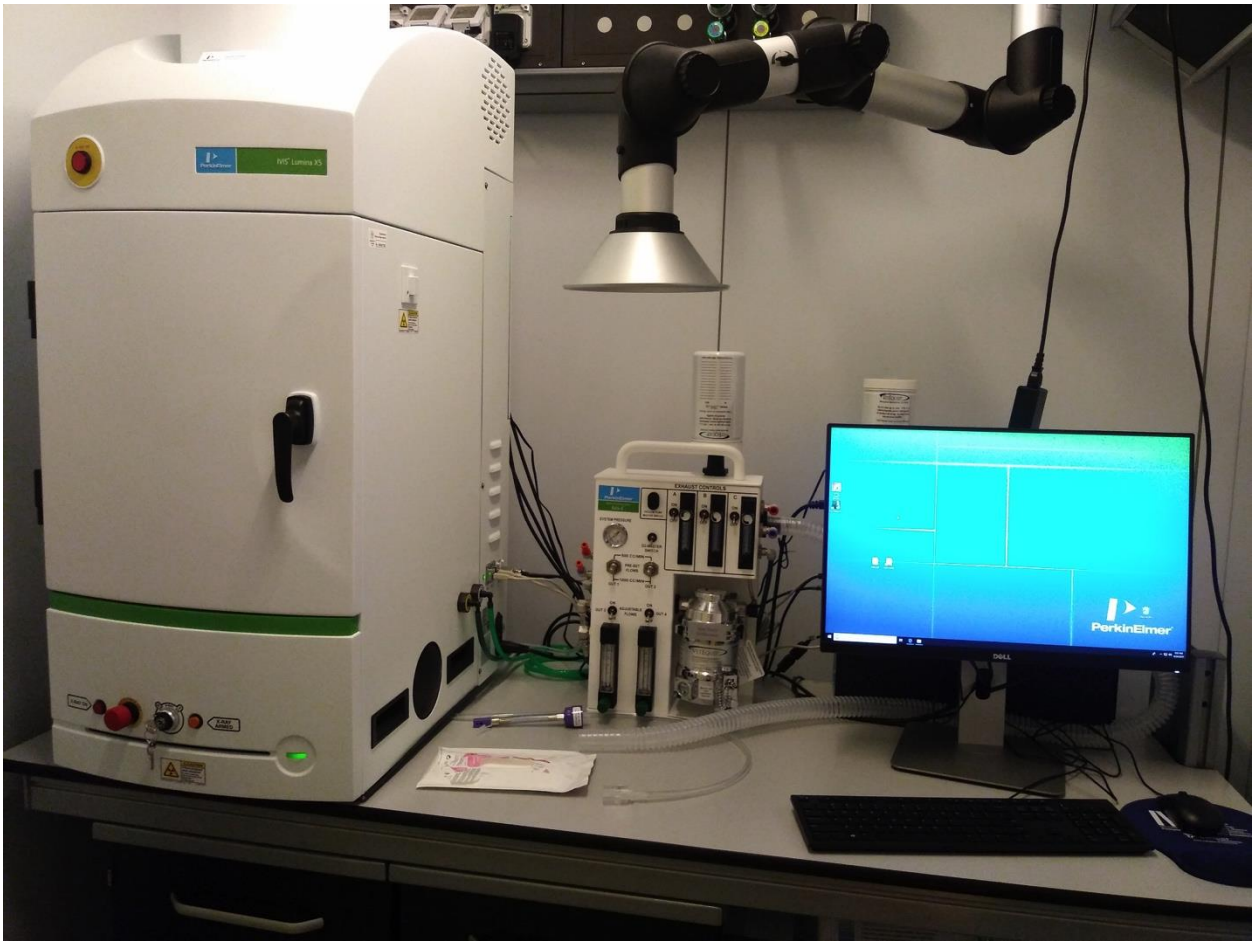

Figure 8. IVIS tool (available at Siena laboratories).

Seven days after the thermogels treatment, mice were treated with 100 µl of luciferin (suggested dosage from maker 30 mg/kg), administered subcutaneusly. Ten minutes after substrate administration, mice were anesthetized with isoflurane and positioned inside the IVIS chamber and kept under anesthesia for the duration of the imaging section. The software allowed recording the luminescence as total radiance: we expressed our results using this value as directly corresponds to the tumor volume. Statistical analysis was performed using the *GraphPad Prism software*.

Results

In vitro characterization of cell models and of smart thermogel features.

MTS assay for the sensitivity analysis of human glioblastoma cell lines to TMZ

The optimization of the method to induce a human glioma into a mouse model started selecting the best human cell line that can recapitulate the main feature of the clinical scenario. We decided to use two different glioma cell lines (U87MG and DBTRG) and verified their sensitivity to Temozolomide (TMZ). IC50 was calculated for the glioblastoma cell lines using a range of 0-1200 μM of chemotherapeutic for 72 hours. As shown in the picture **(Fig.9)**, the curves obtained from the analysis of the MTS assay showed IC50 values for TMZ of145.7 μM for U87MG, while that of DBTRG cells was instead 762.4 μM, confirming the higher sensitivity of the U87MG as found in literature **(Lee, 2016)**. This evidence therefore suggested U87MG cells as the best model to accomplish our purpose and to perform further experiments.

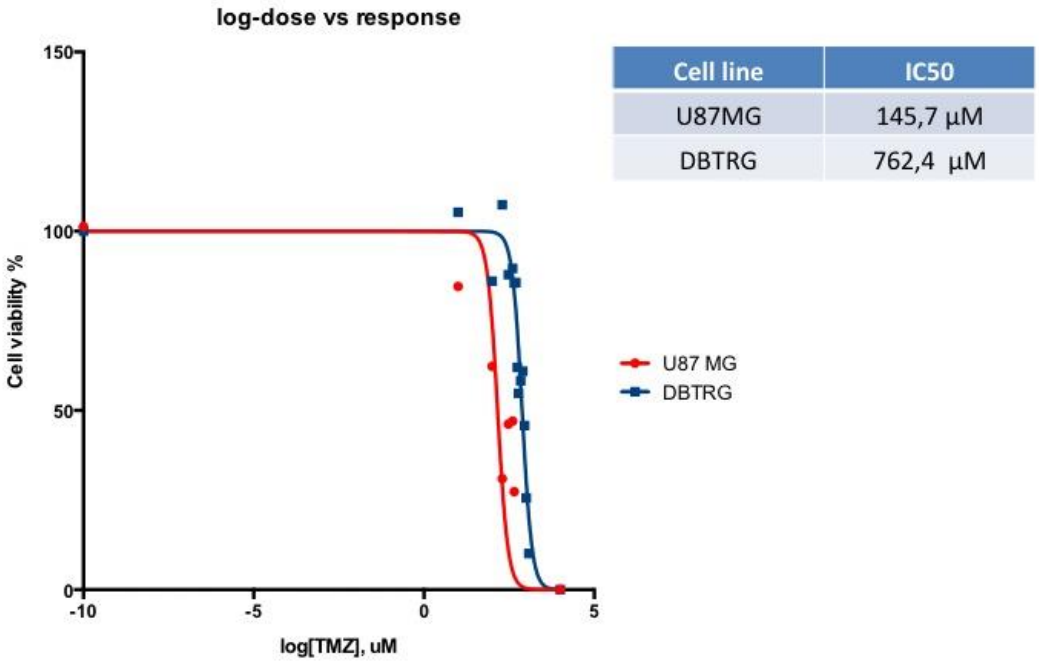

Cell line	IC50
U87MG	145,7 µM
DBTRG	762,4 µM

Figure 9. MTS assay. Dose response curves of U87MG and DBTRG cells after Temozolomide treatment for 72h. IC50 was calculated.

Biocompatibility and release tests

Next, we decided to assess the biocompatibility of the gel that we planned to use for our experiments. This is, in fact, a custom made proprietary thermogel (Bologna University), never tested before on live models: in particular, we wanted to verify not only the biocompatibility but also the manageability and amenability of the smart material: indeed, it is supposed toremain fluid at low temperature but harden at around 37°C. To ensure that the gel itself did not cause any damage *in vitro* to the cells and *in vivo* to the healthy tissue of the brain we conducted a set of *in vitro* and *in vivo* experiment to test gel biocompatibility and toxicity. In particular, we assessed its effect on cell morphology, cell adherence, cell proliferation and cell vitality.

To this aim, we treated the cells for 72 hours with the thermogel in its fluid form and next recovered cells and prepared the samples for optical microscope analysis. For this

experiments, we used U87MG as the bench-mark of glioblastoma *in vitro* model. Cell morphology and cell adherence in U87MG untreated cells (control) versus empty thermogel treated cells were analyzed **(Fig.10A-B)**. We found that the cell morphology was not altered by the gel treatment and cells remained adherent to the flask bottom and viable regardless of the treatment.

To verify the release of TMZ from the gel, we compared the effect of the 72 hours treatment with the empty thermogel and the one with loaded thermogel with TMZ on U87MG, using cell treated with fresh medium as controls. We did not find any significant difference in cell viability between the control and the treated with the empty thermogel samples (Ctrl: $667{,}62x10^3 \pm 1{,}76x10^3$, Empty Gel: $678{,}11x10^3 \pm 6{,}17x10^3$) confirming the biocompatibility of the gel. Instead, a significant reduction in viability was detected when comparing cells treated with empty gel and those treated with gel loaded with TMZ ($616x10^3 \pm 4{,}06x10^3$), confirming the ability of the gel to release the TMZ content and the drug cytotoxicity **(Fig.10C)**.

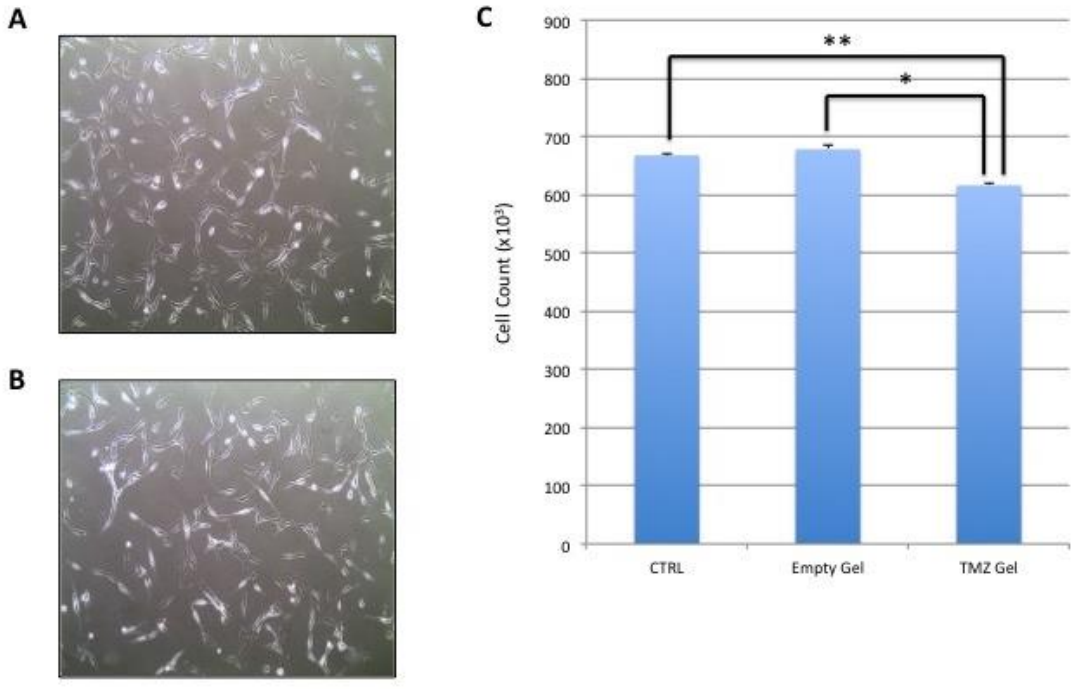

Figure 10. Biocompatibility test of the thermogels: toxicity and release of TMZ. Optical microscopy images of U87MG cells not treated (A) and treated with empty thermogel (B). Statistical analysis. U87MG cell count after treatment with empty thermogel and TMZ loaded thermogel (* 1W.Anova P< 0.05 (C).

Having described the sensitivity of both cell lines and the response of the cells to the thermogel treatment in U87MG, we used this information to build the *in vivo* model for glioma recurrence. However, before starting with the *in vivo* treatment I needed to verify if the gel could be used locally as a neutral, safe, enduring intracranial delivery vehicle for TMZ. That's why at the end of the satisfactory preliminary *in vitro* thermogel studies showing the two main feature needed for the experiment namely cell biocompatibility and TMZ releasing ability, we moved to verify *in vivo* biocompatibility of the smart material.

Biocompatibility test *in vivo*

To this purpose, we needed to apply the gel directly onto the healthy tissue of the brain and leave it in place chronically to reveal any sign of tissue morphological changes or damage/ toxicity. For this, we used the same nude mice model that are will be used in the next xenograft experiments necessary for efficacy tests of the gel loaded with TMZ.
In brief, this procedure includes a micro-drilling craniotomy performed on mice to expose the cranial membrane namely the *Pia mater*, the *Dura mater* as well as the brain tissue underneath. After removing *dura mater*, the gel was placed directly onto the brain tissue. The cranial cap was closed with a replacement membrane of the *dura mater* to avoid liquor loss and the oozing of the gel giving the specific characteristic of the thermo sensibility of the gel that harden at 37°C.We assume that the treatment will stay in place for as long as the gel is reabsorbed by the tissue. After surgery, we monitored mice for a period of 15 days. Then, at the end of the observation period, micro- and macroscopic observation revealed that treated animal brains shows no signs of inflammation or necrosis **(Fig.11A)**, when compared to sham animal, suggesting an excellent biocompatibility of thermogel. The structural integrity of the tissue was verified by hematoxylin-eosin staining **(Fig.11B)**. Moreover, mice showed no weight loss and the general condition were optimal with no macroscopic changes in postural or behavioral motor alterations **(Fig.11C)**. These data prompted us to proceed using the gel in our

experiment, as the use of this agent did not contravene the animal welfare parameter declared in the approved protocol guideline.

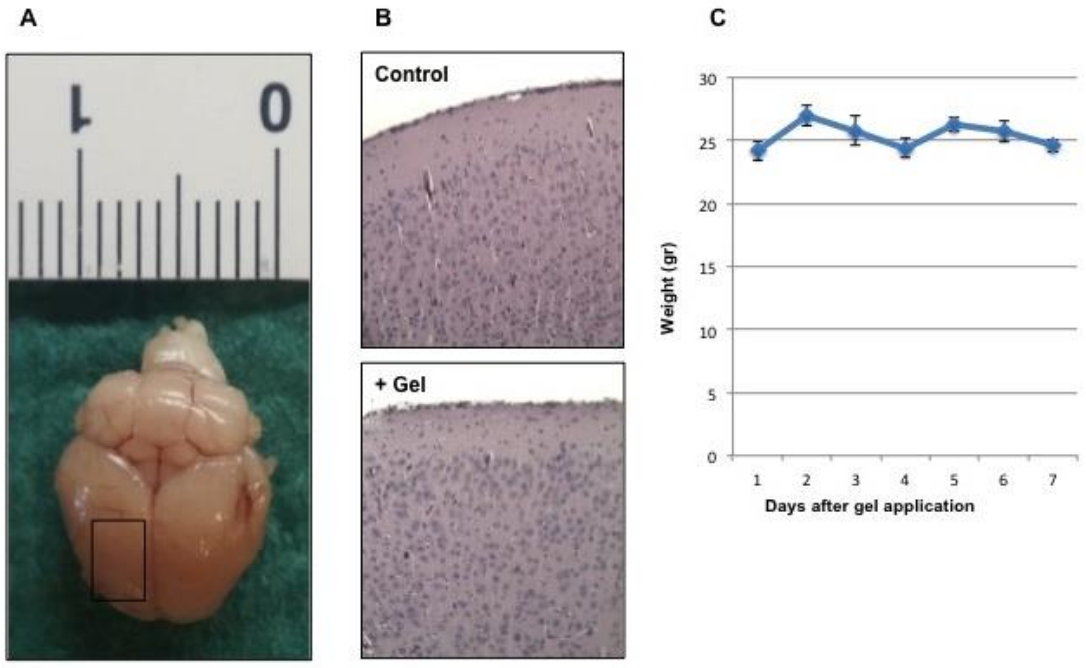

Figure 11. Biocompatibility test of thermogel. Observation of acute and sub-acute local and general toxicity of empty thermogel. After craniotomy and application of empty thermogel, brain explant was performed at day 14 (A). Histological analysis. Comparison of brain tissue after undergoing the craniotomy but without applying the thermogel (control) with that underlying the craniotomy and applying the empty thermogel (+ gel) Colored with hematoxilin–eosin (B). Statistical analysis. Average weights of mice (n=4) after surgical procedure for application of empty thermogel (C).

Cell line, cell concentration, coordinates of inoculation tests

Optimization of the *in vivo* model for the study of the glioma is a major requirement for limiting variability of data and misinterpretation, and to cope with 3R requirement. Therefore, once all the *in vitro* and *in vivo* biocompatibility tests were satisfactory, we proceeded to the development of the mouse model of orthotopic glioblastoma: a series of preliminary implant experiments were conducted choosing respectively two different glioblastoma cell lines, two different concentrations and two different cell inoculum coordinates (see flow chart of activity in **figure 5**).

The first step was to choose the cell line for the intracranial model. U87MG are the benchmark cell line for the preclinical study of glioblastoma, however, in our facilities DBTRG human glioblastoma cell lines were previously used for testing *in vivo* proprietary active molecules giving reliable results. Therefore, we took advantage of this opportunity to screen this cell line for our purpose.

A first set of comparative studies was conducted using both cell lines individually inoculated into the somatosensory cortex of mice. After 18 days from the injections, histological analysis was performed on the explanted brains. Hematoxylin-eosin staining shows that, while the DBTRG cells did not form any visible tumors **(Fig.12a),**U87MG cells induced the development of a clearly visible encapsulated tumor **(Fig.12b)**. Moreover, preliminary data (not shown) demonstrated that DBTRG cells grow extremely slow *in vivo.* We then decided to focus on the use of U87MG, given the good sensitivity measured in our *in vitro* experiment and also from previous published results **(Sun et al., 2004; Salphati et al., 2016)**.

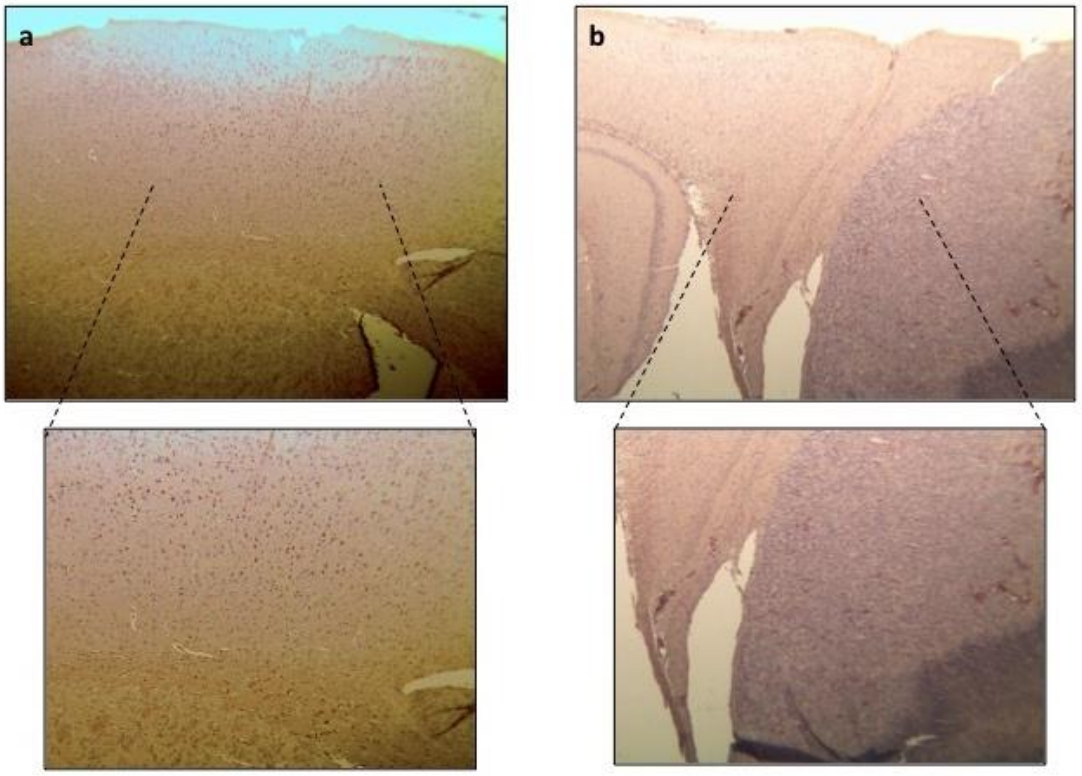

Figure 12. Histological analysis. Hematoxylin-eosin staining of mouse brain sections 18 days post injection of DBTRG (a) and U87MG cells respectively.

The second step was the optimization of cell concentration for efficacy tests of the drug-loaded gel. Our goal was to obtain a tumor whose resection would leave enough cells to induce a relapse, similarly to what usually happens in humans. We therefore decided to test two different tumor cell loads ofU87MG: 2,5 $x10^5$and $5x10^5$ cells. These were inoculated into the somatosensory cortex of immunodeficient mice. After 18 days, tumor growth derived from inoculum of the lower concentration of U87MG cells was not detectable **(Fig.13a)**, while $5x10^5$ cells produced a well-encapsulated measurable tumor mass **(Fig.13b)**.

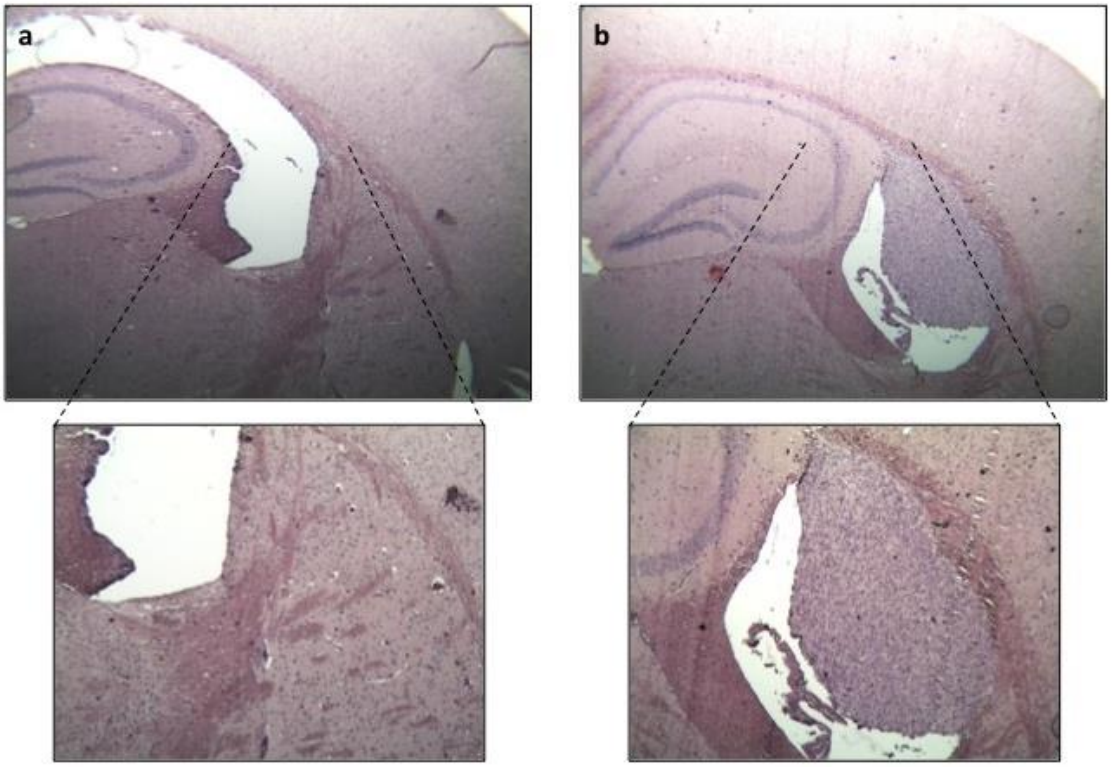

Figure 13. Histological analysis. Hematoxylin-eosin staining of mouse brain sections 18 days post injection into somatosensory cortex of 2,5x10^5 (a) and 5x10^5 U87MG cells respectively.

Another important parameter to take into consideration for the set up of the experiment was the choice of cell inoculation coordinates. To identify the best scenario, two different coordinates sets were tested corresponding respectively more superficially to the somatosensory cortex [(+0.5 mm lateral (x); 1.75 mm antero-posterior (y)] (0.90 mm from the surface deep) or deeper into the striatum (1.90 mm from the surface deep). U87MG cells were injected into these two different areas of the brain and histological analysis were performed 18 days after inoculation. Haematoxylin-eosin staining shows the two tumors clearly visible and encapsulated in the two regions **(Fig.14 a,b)**.

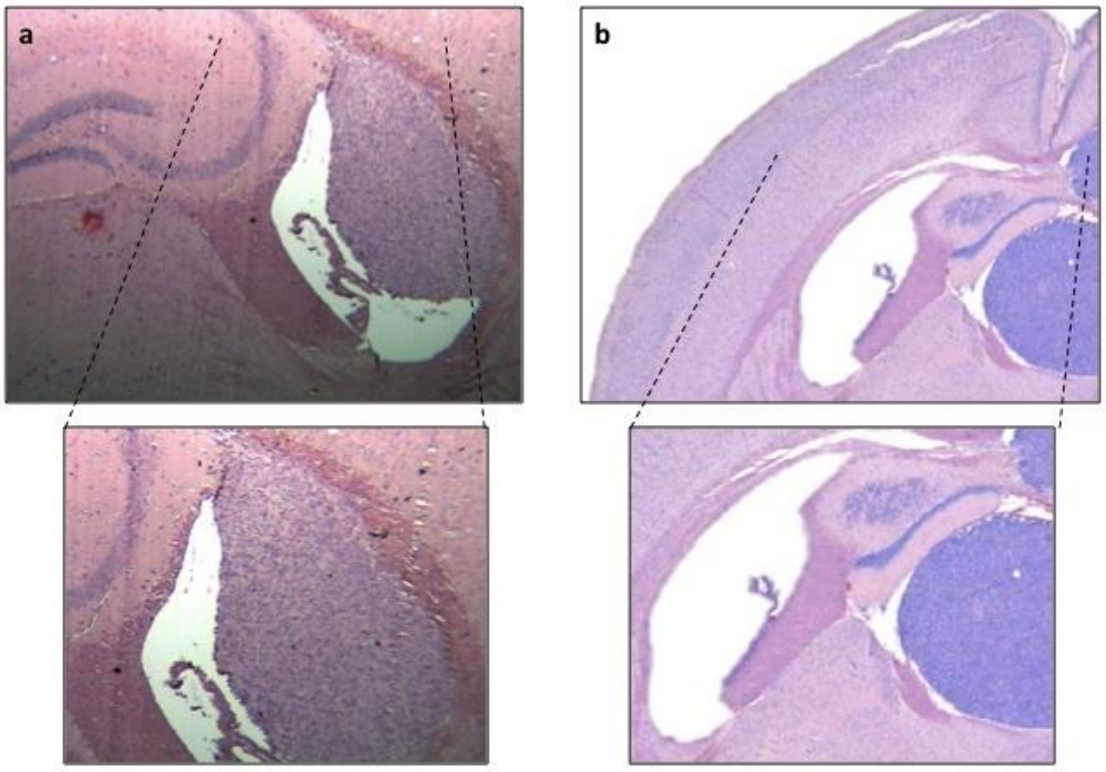

Figure 14. Histological analysis. Hematoxylin-eosin staining of mouse brain sections 18 days post injection of U87MG cells into somatosensory cortex (a) and striatum (b) respectively.

We noticed that while, after injecting the cells into the striatum, tumor growth was mostly confined to tissue region, allowing a wide spreading of the mass and also inducing a visible alteration of the adjacent cerebral structures, the tumor cells injected more superficially into the cortex probably had more chance to reach the void of the ventriculum, reducing the mass formation. As this second possibility would cause a high degree of variability, we therefore decided to continue experiments injecting the cell model into the Striatum, confiding that the strong effect of TMZ could be sufficiently effective on tumors in this subcortical area.

The use of U87MG-Red-FLuc optimizes the experimental design

The Luciferase Assay

The choice of a good cell line model is strategic for the success of the project. The optimization of the model provided us with the best concentration and location for the injection. The choice to use U87MG gave another advantage: the possibility of using a modified luciferin sensitive U87MG model, instrumental for the *in vivo* outcome detection of the intracranial tumor growth. This is the state of the art sensitive imaging method with detection limit as low as emission from few cells, a situation that is virtually impossible to match by proceeding with histological investigation. Moreover, in view of the 3R rules and ethical considerations, *in vivo* detection allowed us to reduce the number of animal used to achieve a significant result.

To verify sensitivity to the light activating substrate of U87MG-Red-FLuc model, a luciferase assay was performed *in vitro*. U87MG-Red-FLuc is stably transfected with and expresses firefly luciferase gene from *Luciola Italica* (Red-FLuc) and is capable of emitting a bioluminescent signal following treatment with the substrate: light is produced by the conversion of the chemical energy of luciferin oxidation into the product molecule oxyluciferin. *In vivo*, bioluminescence is generated when firefly luciferase catalyzes luciferin oxidation using ATP•Mg2+ as a co-substrate, and it is registered as Relative Light Unit (RLU).Here, the *in vitro* bioluminescence assay with U87MG-Red-Fluc human glioblastoma cell line demonstrated intense and robust luciferase activity with subsequent emission. As expected, U87MG cells showed no background luciferase expression **(Fig.15)**.

Once all the preliminary tests were completed and the tumor model was selected, we performed *in vivo* experiments to inject U87MG cells into the striatum of nude mice at the concentration of 5 x 10^5/5 µl of PBS, to generate a suitable model for human glioma to study: 1) the effect of thermogel loaded with Temozolomide on tumor growth and 2) the effect of this treatment on the human glioma recurrence, the latter using U87MG-Red-FLuc.

Cell line	RLU
U87MG	10063
U87MG-Red-FLuc	13917252

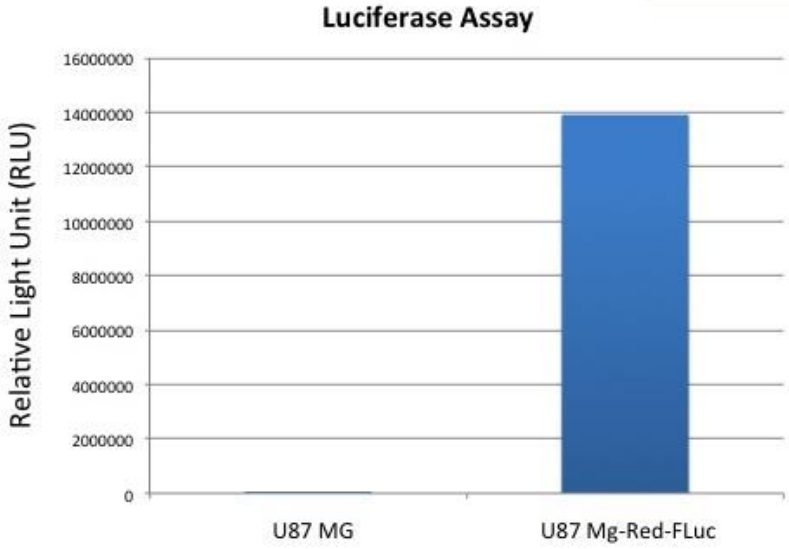

Figure 15. Luciferase assay. Luciferase expression (RLU) in U87MG cells and U87MG-Red-FLuc cell line which was transfected with firefly luciferase gene from Luciola Italica (Red-Fluc).

1) The effect of the thermogel on glioblastoma growth

U87MG cells were injected as described above and we estimated that seven days after the injection into the brain tissue, the tumor mass had reached a suitable volume. At this point, the procedure included the opening of a cranial window on the skull of each animal to place the thermogel in contact with the open surface of the affected area to induce a local delivery.

After histological investigation, we found that, in animals treated with the empty thermogel **(Fig.16A)** the tumor spread into the subcortical area often reaching the area of the bordering ventricles, altering the morphology of the surrounding brain tissue. On the other hand, when the brain from mice treated with loaded thermogel was observed **(Fig.16B)**, the growth and infiltration of the tumor were limited to the areas around the injection site. Measuring the maximum area of the tumor on the coronal sections of the brain **(Fig.16D)** we found that, overall, there was a significant reduction of growth in the group treated with gel+TMZ when compared to the control group (empty gel: 4,58±0,41;

TMZ gel: 1,63±0,60). Observational evaluation of the general condition of the mice confirmed that the application of the gel did not induce macroscopic alterations, as the control group did not show any weight loss, postural or behavioral motor changes **(Fig.16C)**.

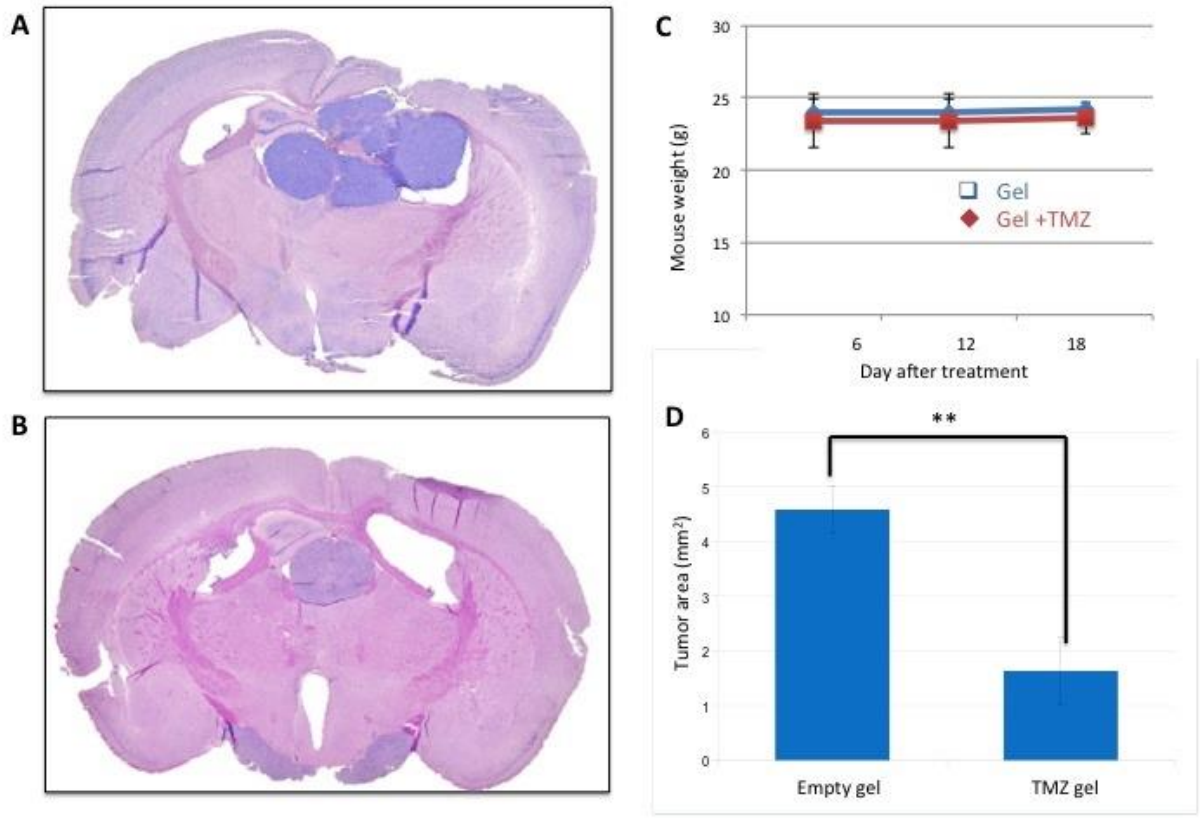

Figure 16. Histological analysis. Hematoxylin and eosin staining 10 days post injection of U87MG cells and treatment with empty thermogel (A) and thermogel lcontaining Temozolomide (B) respectively. Control of the general condition of the animals. Weight control of mice after thermogels treatment. Weigh every four days (C). Statistical analysis. Measurements of the glioblastoma area in mice treated with empty thermogel and with thermogel containing Temozolomide (T-test p<0,001) (D).

2) The time course and effect of the new gel treatment on glioblastoma recurrence

From the previous experiment, we concluded that the treatment with loaded gel+TMZ indeed retards tumor mass growth in mice. We then proceeded to modeling the surgical

procedure to remove the tumor mass, to closely mimic a clinical set of surgical intervention. This procedure allowed the study of glioma recurrence, a situation often observed in patients after initial surgical treatment. As described above, to this purpose $5x10^5$ U87MG-Red-FLuc human glioblastoma cells expressing luciferase were injected into the *striatum.* Seven days after cellular inoculation, a craniotomy was performed allowing the opening of a cranial window to access and partially remove the underlying tumor mass by using a biopsy punch. This surgical step therefore removed most tumor cells (residual cells would then give rise to tumor relapse) while creating a cavity onto the brain parenchyma where the gel could be easily lodged. After tumor removal, animals were treated individually either with empty or TMZ loaded gel. Importantly, the use of the U87MG-Red-FLuc cells allowed observation, by life imaging, of the effect of each treatment on alive animals, recording different time-points of tumor growth after thermogel treatment.

The bioluminescence signal captured by IVIS (live imaging luciferase-based instrument) at the end of the treatment and analyzed off line, clearly showed that a 7 day local treatment with loaded gel significantly limited the recurrence of tumor growth (empty gel: $83408x10^5 \pm 30912x10^5$; TMZ gel: $16575x10^5 \pm 6424x10^5$) **(Fig.17)**.

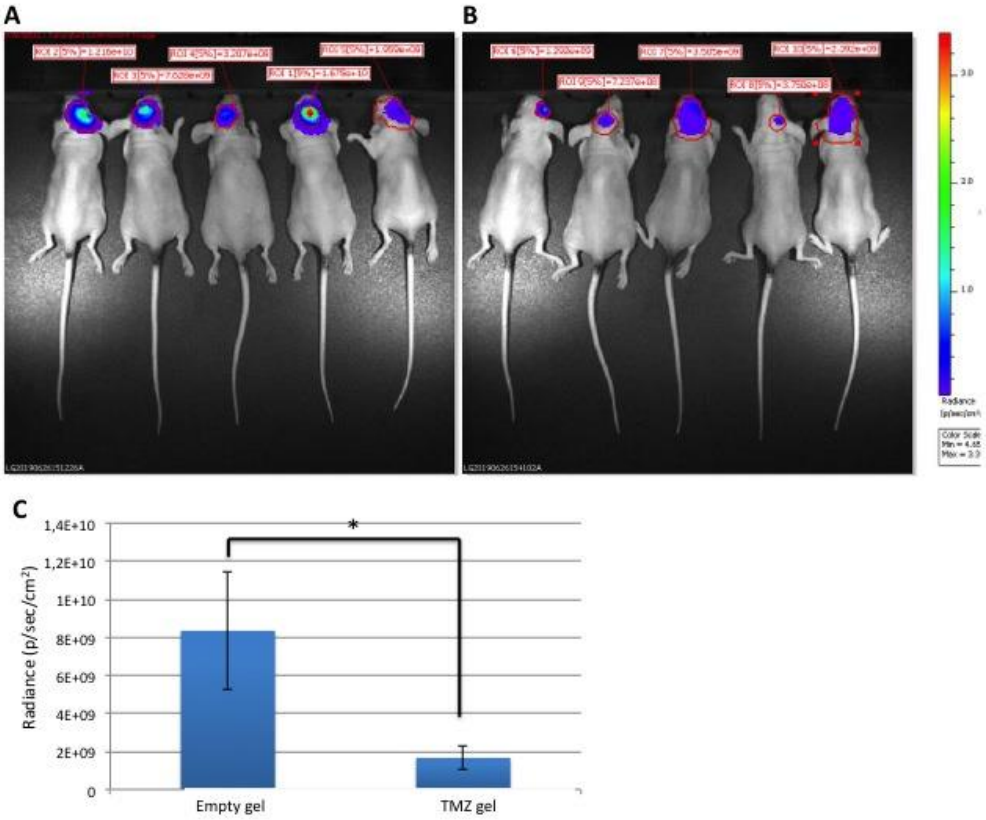

Figure 17. IVIS analysis. Measurement of the fluorescence intensity of U87MG-Red-FLuc cells injected into the striatum after 7 days of treatment with empty thermogel (A) and with thermogel containing Temozolomide (B). Statistical analysis. Analysis of the luminescence (radiance) of the ROIs in mice treated with empty thermogel and with thermogel containing Temozolomide (t test = p ≤0.05) (C).

Discussion

The main goal of my thesis was to develop a reliable model for the study of recurrences of human glioblastoma in nude mice model. Moreover we aimed to exploit the possibility of using a therapeutic formulation based on a thermo-sensitive gel containing a benchmark chemotherapeutic to verify the potential of the "smart" gel as an antitumor local therapy. We successfully managed to create an intracranial tumor model using U87MG Red-FLuc human modified cells, widely used in literature to study the characteristics of human glioma both *in vitro* and *in vivo*. We were also able to obtain a reduction in tumor progression and recurrence using a new technique of primary tumor mass resection in animal treated with a local intracranial therapeutic gel deposition. A similar attempt to create a resection model was already described **(Bianco et al., 2017)**, showing that recurrences were reduced and animal life was slightly prolonged in animals that received surgical punch resection. A similar technique was used in Sheets et al. **(2018)** for the local implantation of a curative scaffold of PLA loaded with mesenchimal stem cells (MSC), exploiting the regenerative potential of MSC to salvage to brain tissue. Here, I exploited the potential of the cavity created by the surgical punch to accommodate around 10 µl of thermo-reactive curative gel, able to solidify at body temperature, to significantly reduce the growth of glioma recurrences. Our experimental endpoint did not included the animal death, as required by the 3R Guidelines and suggested by the local Animal Welfare Body (AWB), and no significant signs of distress were visible in either of the two groups at time of sacrifice.

To optimize this protocol and validate the technique I could rely on stepwise improvements to the accomplishment of the goal.

As literature extensively shows, the U87MG cell line is the benchmark model for the study and *in vivo* development of glioblastoma. However, we have performed several studies on two different human glioblastoma cell lines (U87MG and DBTRG) to evaluate their characteristics and choose the best one for our specific aims. We first evaluated cell growth *in vitro*. In fact, although this parameter does not reflect the growth that cells can have when inoculated in animals, it can give us good indications on how to proceed

in the implant in the brain. In our case, the two cell lines examined had a very similar growth rate, so our choice was guided by the analysis of other parameters. We also wanted to check the sensitivity of the two cell lines to TMZ. Since the final aim of this project was to develop a smart material to improve delivery of efficacious chemotherapy (and TMZ is the first line treatment for GBM patient to date) it was mandatory to choose a TMZ sensitive cell line. The results confirmed the data published by Lee **(2016)**, showing the sensitivity of the U87MGcells for this chemo-drug that induced strong cell mortality, unlike the DBTRG cell line, for which a much higher IC50 was detected. Moreover, the DBTRG model previously employed in our lab showed a slow growth rate and recurrences appearance, a situation that did not satisfy the requirement for the gel application and leave-in-place. In addition, the possibility of following the intracranial growth of luciferase modified U87MG by live imaging (IVIS) and strongly reducing the number of animals employed for the study and the suffering (refinement) encouraged us to select U87MG for a valid comparison. Specifically, U87MG-Red-FLuc model is extremely reliable and the IVIS imaging system is guaranteed to be highly sensible to the presence of small amount of intracranial luminescent cells. To make sure we had the best tumor model and that the commercially available cell line, U87MG-Red-FLuc, provided bioluminescence strong enough to be detected by IVIS, we performed a luciferase assay. The positive results obtained from this assay provided confirmation of the sensitivity of this cell line. This feature was fundamental for us to be able to follow the growth of the tumor inside the brain without being forced to sacrifice the animals at each time-point. Indeed, imaging of intracranial areas is quite tricky, given the tough skull bones barrier protecting the inner tissues. In a previous project on glioma in the lab, we planned to use ultrasounds (VEVO imaging system) to verify cerebral lesions, but it was impossible to achieve a clear readout of the tumor mass growing inside the brain. The MRI system is a valid alternative method that many authors use for the study of intracranial glioma **(Shukla et al., 2017)**. I opted for the use of IVIS counting on the amenability and minimal impact of the luciferase administration of the well being of the animal, according to our approved protocol that did not included the possibility of administration of a opaque contrast agent that could interfere with the presence of the curative gel. All these factors, i) the greater sensitivity to Temozolomide, ii) the best

engraftment *in vivo* and iii) the immediate availability of a line with luciferase, led us to choose U87MG as the human glioblastoma cell line for the development of the recurrence model of glioblastoma in mice and it allowed a more accurate and precise analysis of tumor growth.

The innovative part of this project was the use of smart materials. Smart materials have risen increasing attention in the biomedical research fields thanks to their adjustable physical and/or chemical properties in response to deliberately imparted external stimuli or to environmental changes. For these reasons, their introduction in nanomedicine has opened unprecedented possibilities of manipulation of biological entities at cellular and even sub-cellular level **(Genchi et al., 2017)**. Today's treatment of glioblastoma confined to the use of rigid Gliadel “wafers” loaded with Carmustine necessitates the development of more effective nanomaterials against tumor recurrence **(Ashby et al., 2016)**. In fact, the limit of this treatment is the consistency of the “wafer”, in addition to the use of Carmustine, a quite obsolete chemotherapeutic. The rigidity of the “wafer” prevents this device from adhering perfectly to the cranial cavity formed by the surgical removal of the tumor. This represents a big limitation as the drug cannot reach and kill the cancer cells left in place. It is therefore evident the need to develop a material with a suitable consistency to completely fill the cavity formed by surgery and which can be loaded with a more effective drug. For these reasons, we decided to use a thermogel produced by the University of Bologna as carrier to deliver a chemo-drug to the brain. The interesting feature of these thermogels is their reverse gelation ability. In fact, they are in the liquid state at low temperatures (4°C) while they gelatinize when body temperature (37°C) is reached **(Patel et al., 2018)**. This peculiarity makes these materials easier to handle than other carriers. In fact, this thermogel can be easily handled in the liquid form at 4°C, then administered with extreme precision with a pipette inside the cavity, where it will adhere perfectly to the walls of the remaining cancer cells (responsible for recurrence), filling every space. Once the temperature is reached, the thermogel hardens, allowing the matrix to remain in place and not to escape from the cavity, and locally release TMZ in a semi-controlled fashion. Not to risk infection or

toxicity we confirmed the biocompatibility of the material by comparing the treated cells with the controls, and ascertained their viability and proliferative capacity by cell count.
The next step was to verify the ability of this material to gradually release its content to its exterior. This characteristic was fundamental for the success of the treatment, so we asked our collaborators in Bologna to load a thermogel, of identical composition to the empty one, with TMZ, the chemo-drug we wanted to use in our project. The advantage of using a smart material like this thermogel lies in being a hydrogel, a polymeric material that has the ability to absorb >20% of its weight of water and still maintain a distinct 3D structure **(Gupta et al., 2002)**. Traditionally, controlled-release designed polymeric systems have been classified into 'matrix' and 'reservoir' types **(Langer, 1980)**. Matrix systems are most commonly employed because of their ease in development, cost-effectiveness and better performance. However, these systems tend to follow Higuchi's model, wherein drug release is proportional to the square root of time (t½). This leads to non-uniform release rates, continuously decreasing in the beginning and more rapidly thereafter. The key benefit of hydrogels for controlled drug delivery lays in the near constant release rates.
This was described in our experiments, by comparing the loss of the viability and proliferative capacity of cell treated with loaded and empty control gel, by cell counting. The *in vitro* gel/TMZ activity profile acquired up to here was mandatory to proceed optimizing the use of TMZ loaded thermogel for *in vivo* study.
This was a very long phase of development to obtain the animal relapse model of human glioblastoma similar to the clinical condition of patients suffering from this tumor.
For the patients to benefit, these systems are placed in direct and sustained contact with the tissues, and some of them degrade in situ. Thus, both the material itself and its degradation products must be devoid of toxicity. We were concerned that the biocompatibility of an implanted material relies on various parameters depending on the host and on the material itself **(Fournier et al., 2003)**. Many parameters impinge on material stability and integrity, that may depend on the physical/chemical state of the material (like shape, size, surface chemistry and roughness, design, morphology and porosity, composition, sterility issues, contact duration and degradation) however some factors are not directly related to the matrix such as the species, the genetic inheritance,

the site of implantation, and the microenvironment, **(Laurencin et al., 1994; Babensee et al., 1998)**.

For this reason it was necessary to validate the gel application on the model, in absence of tumor, to check on intrinsic toxicity *in vivo* of these materials. To carry out this type of test we had to develop a protocol to perform a craniotomy to expose a part of the brain corresponding to the tumor. This allowed us to place the thermogel directly in contact with the brain tissue and to ensure matrix biocompatibility. The craniotomy procedure was performed following the indication of Goldey et al. for the formation of a cranial window for long-term imaging **(Goldey et at., 2014)** and we used a mini drill to perform it. However during the process we faced the need for an intense activity of troubleshooting: for example we needed to limit fast drilling to avoid over heating as well as bleeding from brain capillaries. At the same time we experimented Duraform as a possible *Dura* replacement after gently using the forceps to remove loose bones from the cap after craniotomy. Surgical glue was also used instead of previously employed stitches serious damage to the underlying brain. It was essential to keep the thermogel on ice during the whole procedure. As mentioned above, in fact, the gel at low temperatures is in liquid form and this facilitated the gel to be carried and placed using a pipette to gently lay it on the brain tissue. When a cavity was created (during the treatment experiment with tumor removal) the tricky part was to fill the void with gel. For all these steps adequate histological analysis carried out confirmed the quality of surgical operation and the biocompatibility of the material *in vivo* and allowed us to proceed with the development of the tumor model.

To this day, surgical resection remains as the main component in treating GBM. However, the focus of most preclinical models is on treating established tumors, with only a limited number of animal models currently available that focus on resecting tumors. In view of this shortage, we developed a novel, simplified and reproducible intracranial resection mouse model. Although the *in vitro* experiments directed us towards the use of the U87MG cell line, we still wanted to test the DBTRG cell line *in vivo*, to ensure the use of the best line. In fact, it is not obvious that a line that is cultivated well *in vitro* takes root equally well *in vivo*. The aim was to develop a tumor

inside the brain that would grow encapsulated to prevent growth spread throughout the brain. Even though we used the non-invasive U87MG cell for tumor formation, the purpose of this study was to develop a resection and recurrence model that could be implemented in varying treatment modalities for GBM. In fact, the resulting resection cavity allowed us to investigate novel treatment strategies based on local delivery of TMZ encapsulated in hydrogels for local delivery of anti-cancer agents, permitted by their unique properties.

In our case, we needed to recreated a virtual-clinical situation in which local deliver could be performed with a persistent support directly on the brain, from where it would have released TMZ: the tumor could not be too deep, otherwise the drug would hardly have reached the site and exert little or no effect: in this case we would have consider a false negative result (no effect even if the gel did released the TMZ). On the other end, if the inoculum was too superficial, cells might have been extruded toward outside by Hamilton syringe pressure at time of removing the needle from site of seeding or being misplaced within the skull, when creating the cranial window, and tumor development could be underestimated. Because of these issues, we tried to inoculate tumor cells in the striatum, a subcortical region of the brain. In this way, we verified that the tumor was deep enough not to attach to the skull but not too much not to be reached by the gel. Furthermore, we also reduced the risk of leakage of the inoculated cells, in fact being inoculation point much deeper than the previous cortical one we were able to remove the Hamilton slowly without unwanted cell leakage.

To this point and for the setting of the model we rely on histology to assess the effect of thermogel and TMZ on glioblastoma growth reduction. In fact the U87 cell line we used were not endowed with any “beacon” to shed light where the cells were located.

Histology is a classic technique widely used in pathology and probably still the most spread mean of investigation, however it comes with some issues: a full study it requires an elevated number of animals to achieve a significant result in a chronic study similar to the one we carried for this investigation. Moreover the post mortem processing and the specimen preparation require long time as in our case, from brain collection to imbedding to obtain a good histological preparation **(Paradiso et al., 2018)**, and finally cutting **(Zhang et al. 2014)**, and histological processing.

We performed our fixation so that hematoxylin and eosin staining allowed us to clearly distinguish the tumor from the surrounding healthy brain tissue and, using Nikon microscopy control software (NIS 2.3) we were able to delimit the tumor mass and calculate the area of glioblastoma for each slice. In this way it was possible to compare the areas of the tumors of the mice treated with the empty thermogel with those of the tumors of the mice treated with the gel containing TMZ.
In our case, to initial accommodation of the animals in their cage to the data analysis of histology data the whole process may last for almost 2 months.

For all the limiting factors we detailed, and having the possibility of using both glioblastoma cells stably expressing luciferase (U87MG-Red-FLuc supplied by Perkin Elmer), we set up the subsequent experiments differently. In recent years, the use of machinery such as IVIS to record bioluminescence has been growing. In fact, this type of analysis allows to use fewer animals in *in vivo* studies and to have much more precise measurements and therefore to be able to monitor tumor growth **(Alharbi et al., 2019)**. Moreover in our case, histological analysis represented a solid basis for verifying their efficacy at the end of the treatments, but could not be used for monitoring the growth of the tumor mass unless using a huge number of animals (countervening the 3R requirements). IVIS could be used also to detect fluorescence signaling, however fluorescence imaging requires strategies to accurately compensate for mechanistic or non-mechanistic fluorescence background; signal is derived from systemic injection of these probes which will generate target signal as well as signal in sites of probe metabolism or non-target sites of mechanistic biomarker expression. Without proper fluorescence background comparison or subtraction, results may underestimate biological changes or the magnitude of therapeutic efficacy, whereas excessive background compensation can reduce sensitivity in the detection of lower intensity fluorescence changes. Therefore we opted for the bioluminescence mode.
The last aspect that validates the protocol was to standardize the tumor removal. The use of the biopsy punch for the removal of the tumor mass was has been used before **(Bianco et al., 2017)** and it fundamental in order to create a cavity in the brain where the thermogel could be inserted avoiding escaping and scattering around on the healthy

brain tissue. Indeed, the proper placement of the gel will protect the functional tissue (healthy neurons) from the secondary side effects of TMZ, which is a chemotherapeutic with a relative small therapeutic window, often administered as coadjutant and concomitant therapy after radiation. Our preliminary trials showed that the height of the biopsy punch blade was too high, as the tool was originally designed to act on for thicker tissues (skin/derma, **Chopra et al., 2015**). So, in order to avoid cutting the brain too deeply, we used silicone circles (i.e. one or more lock washers) to reduce the playing height of the punch, adding a specific “artisan” intervention to the protocol. This allowed us to be able to cut the piece of brain corresponding to the tumor by only a couple of millimeters, avoiding brain damage. In future, we will 3D print proper robber lock washers for our punch that will fit different requirements.

All the phases of the optimization of the standard protocol we adopt for this study will allow an unbiased comparison of future results. Moreover we strictly managed to adhere to the 3R requirement of reduction, replacement, refinement: reduction was implemented by moving towards the use of U87MG Red-FLuc cell line, to limit the number of animal employed to achieve significant results. Replacement was implemented by exploiting as much as possible the information obtained by *in vitro* experiments, thoroughly performed to unveil all possible hidden problems. Refinement, consisting in all those intervention aimed at minimizing the pain caused to animals, was applied both during the experiment, using appropriate painkiller and antibiotic treatment at post surgery and at time of sacrifice, when animals were euthanized after isofluorane induction.

Conclusions

To date, there is still not a definite answer to the difficulties encountered in being able to offer effective treatment for Glioblastoma multiforme (GBM), the most aggressive and most frequent neoplasm among those that originate from the cerebral nervous system. For this tumor located inside the brain and above the blood-brain barrier the frequency of recurrences leads to a dismal prognosis in humans. Moreover, the encouraging results obtained with new drugs on glioma cell lines, laying in the pharmaceutical R&D pipelines are utterly minimized by the presence of the BBB, when administered systemically.

All these considerations prompted us to develop this research project for an alternative vehicle for locally delivering anti tumor drugs for the cure of GBM. We were able to develop a new treatment strategy based on the use of a smart carrier for the release of a chemotherapeutic agent into the brain to counteract the recurrence of GBM. I have developed a recurrence model of mouse GBM that reflects the human clinical status. In addition, I have optimized a protocol of brain microsurgery and partial removal of the tumor mass. These two procedures also allowed me to use thermogel, a smart material for an effective treatment of GBM with TMZ, overcoming the limitations of applying a rigid matrix as in today's GBM treatment that occurs following the surgical removal of the tumor, in the effort to allow TMZ to reach the highest possible number of cells that inevitably will be left behind after tumor removal. This new developed technique of local delivery might improve the low treatment efficiency of TMZ that is however the current first choice treatment for after surgery in human.

Ultimately, we therefore managed to standardize a protocol to obtain an encapsulated tumor, to be able to perform precision surgical resection to show recurrence re-flourishing This can allow the study of countless treatments, from the different types of vehicles, and can be implemented for the study of a variety of molecule, as long as they are encapsulated, linked or even loaded into the matrix. This method can therefore open the way to other future preclinical experiment and finally clinical trials.

Given the encouraging results obtained in this project, further studies will be performed testing the potential of different smart materials and different anticancer agents and the use of thermogel as a smart carrier represents a great advantage in terms of treatment and administration. Finally the goal is to obtain effective treatment that extends the life expectancy of patients with GBM, who are nowadays hopeless.

References

Aderibigbe BA. *In Situ-Based Gels for Nose to Brain Delivery for the Treatment of Neurological Diseases.* Pharmaceutics 2018; 10(2): 40.

Alharbi M, Lai A, Guanzon D, Palma C, Zuñiga F, Perrin L, He Y, Hooper JD, Salomon C. *Ovarian cancer-derived exosomes promote tumour metastasis in vivo: an effect modulated by the invasiveness capacity of their originating cells.* Clin Sci (Lond) 2019; 133 (13): 1401-1419.

Anton K, Baehring JM, Mayer T. *Glioblastoma multiforme: Overview of current treatment and future perspectives.* Hematol Oncol Clin North Am 2012; 26: 825-53.

Attenello FJ, Mukherjee D, Datoo G. *Use of Gliadel (BCNU) Wafer in the Surgical Treatment of Malignant Glioma: A 10-Year Institutional Experience.* Ann. Surg. Oncol. 2008; 15: 2887-2893.

Ashby LS, Smith KA, Stea B. *Gliadel wafer implantation combined with standard radiotherapy and concurrent followed by adjuvant temozolomide for treatment of newly diagnosed high-grade glioma: a systematic literature review.* World J Surg Oncol. 2016; 14(1): 225.

Babensee JE, Anderson JM, McIntire LV, Mikos AG. *Host response to tissue engineered devices.* Adv Drug Delivery Rev 1998; 33: 111-39.

Bastiancich C, Danhier P, Préat V, Danhier F. *Anticancer drug-loaded hydrogels as drug delivery systems for the local treatment of glioblastoma.*Journal of Controlled Release 2016; 243: 29–42

Begley DJ. *ABC transporters and the blood–brain barrier.* Curr Pharm Des.2004; 10(12): 1295-312.

Begley DJ, Pontikis CC, Scarpa M. *Lysosomal storage diseases and the blood–brain barrier*. Curr Pharm Des. 2008; 14(16): 1566-80.

Bellettato M, Scarpa M. *Possible strategies to cross the blood–brain barrier.* Italian Journal of Pediatrics 2018; 44(Suppl 2): 131.

Beroukhim R, Getz G, Nghiemphu L, Barretina J, Hsueh T, Linhart D, Vivanco I, Lee JC, Huang JH, Alexander S, Du J, Kau T, Thomas RK, Shah K, Soto H, Perner S, Prensner J, Debiasi RM, Demichelis F, Hatton C, Rubin MA, Garraway LA, Nelson SF, Liau L, Mischel PS, Cloughesy TF, Meyerson M, Golub TA, Lander ES, Mellinghoff IK, Sellers WR. *Assessing the significance of chromosomal aberrations in cancer: Methodology and application to glioma.* Proc Natl Acad Sci USA 2007; 104:20007–12.

Bianco J, Bastiancich C, Jankovski A, Des Rieux A, Préat V &Danhier F. *On glioblastoma and the search for a cure: where do we stand?* Cellular and Molecular Life Sciences 2017; 74: 2451-2466.

Brem H, Piantadosi S, Burger PC. *Placebo-Controlled Trial of Safety and Efficacy of Intraoperative Controlled Delivery by Biodegradable Polymers of Chemotherapy for Recurrent Gliomas.* The Polymer-brain Tumor Treatment Group. Lancet 1995; 345: 1008-1012.

Chaudhary PM, Roninson IB. *Expression and activity of P-glycoprotein, a multidrug efflux pump, in human hematopoietic stem cells.* Cell 1991, 66: 85-94.

Chen J, Li Y, Yu TS, McKay RM, Burns DK, Kernie SG, Parada LF.*A restricted cell population propagates glioblastoma growth after chemotherapy*. Nature 2012; 488: 522–6.

Chopra K, Calva D, Sosin M, Tadisina KK, Banda A, De La Cruz C, Chaudhry MR, Legesse T, Drachenberg CB, Manson PN, Christy MR.*A comprehensive examination of topographic thickness of skin in the human face.*AesthetSurg J 2015; 35(8): 1007-13.

Clarke J, Butowski N, Chang S. *Recent advances in therapy for glioblastoma.* Arch Neurol 2010; 67: 279-83.

Day SE, Waziri A. *Clinical trials of small molecule inhibitors in high-grade glioma.* Neurosurg Clin N Am 2012; 23: 407- 16.

Drablos F, Feyzi E, Aas PA, Vaagbo CB, Kavli B, Bratlie MS, Peña-Diaz J, Otterlei M, Slupphaug G, Krokan HE. *Alkylation damage in DNA and RNA repair mechanisms and medical significance.* DNA Repair (Amst) 2004; 3: 1389- 407.

Fournier E, Passirani C, Montero-Menei CN and Benoit JP. *Biocompatibility of implantable synthetic polymeric drug carriers: focus on brain biocompatibility.* Biomaterials 2003; 24: 3311-3331.

Genchi GG, Marino A, Tapeinos C and Ciofani G. *Smart Materials Meet Multifunctional Biomedical Devices: Current and Prospective Implications for Nanomedicine.* Front BioengBiotechnol. 2017; 5: 80.

Goldey GJ, Roumis DK, Glickfeld LL, Kerlin AM, Reid RC, Bonin V, Schafer DP, Andermann ML. *Removable cranial windows for long-term imaging in awake mice.* Nature protocols, 2014; 9:11.

Gupta P, Vermani K, Garg S. *Hydrogels: from controlled release to pH-responsive drug delivery.* DDT, 2002; 7: 10.

Harder BG, Blomquist MR, Wang J, Kim AJ, Woodworth GF,Winkles JA,Loftus JC, Tran NL.*Developments in Blood-Brain Barrier Penetrance and Drug Repurposing for Improved Treatment of Glioblastoma.*Front Oncol 2018; 8: 462.

Hart MG, Grant R, Garside R, Rogers G, Somerville M, Stein K. *Chemotherapeutic wafers for High Grade Glioma.* Cochrane Database Syst Rev 2008; 3:CD007294.

Karim R, Palazzo C, Evrard B, Piel G. *Nanocarriers for the treatment of glioblastoma multiforme: current state-of-the-art*, J. Control. Release, 2016; 227: 23-37.

Langer R.*Polymeric delivery systems for controlled drug release.* Chem. Eng. Commun., 1980; 6: 1-48.

Laurencin CT, Elgendy H. *The biocompatibility and toxicity of degradable polymeric materials: implications for drug delivery.* In: Domb AJ editor. Polymeric site-specific pharmacotherapy. New York; John Wiley & Sons Ltd, 1994; 27-46.

Lee SY. *Temozolomide resistance in glioblastoma multiforme.* Genes & Diseases, 2016; 3: 198-210.

Lin CC, Metters AT. *Hydrogels in controlled release formulations: network design and mathematical modeling.* Adv. Drug Deliv. Rev. 58, 2006: 1379-1408.

Liu G, Akasaki Y, Khong HT, Wheeler CJ, Das A, Black KL, Yu JS. *Cytotoxic T cell targeting of TRP-2 sensitizes human malignant glioma to chemotherapy.* Oncogene 2005; 24: 5226-5234.

Louis DN, Ohgaki H, Wiestler OD, Cavenee WK, Burger PC, Jouvet A, Scheithauer BW, Kleihues P. *The 2007 WHO classification of tumours of the central nervous system.* Acta Neuropathol 2007; 114:97-109.

McGirt MJ, Than KD, Weingart JD, Chaichana KL, Attenello FJ, OliviA, Laterra J, Kleinberg LR, Grossman SA, Brem H, Quiñones-Hinojosa A. *Gliadel (BCNU) wafer plus concomitant temozolomide therapy after primary resection of glioblastoma multiforme.* J Neurosurg 2009; 110: 583–8.

Muldoon LL, Alvarez JI, Begley DJ, Boado RJ, Del Zoppo GJ, Doolittle ND, Engelhardt B, Hallenbeck JM, Lonser RR, Ohlfest JR, Prat A, Scarpa M, Smeyne RJ, Drewes LR, Neuwelt EA. *Immunologic privilege in the central nervous system and the blood–brain barrier.* J Cereb Blood Flow Metab. 2013; 33(1): 13-21.

Ohgaki H, Kleihues P. *The definition of primary and secondary glioblastoma.* Clin Cancer Res 2013; 19: 764- 72.

Paradiso B, Simonato M, Thiene G, Lavezzi AM. *From fix to fit into the autoptic human brains.* European Journal of Histochemistry 2018; 62: 2944.

Pardridge WM. *The blood–brain barrier: bottleneck in brain drug development.* NeuroRx. 2005; 2(1): 3-14.

Patel M, Lee HJ, Park S, Kim Y, Jeong B. *Injectable thermogel for 3D culture of stem cells.* Biomaterials. 2018; 159: 91-107.

Peppas NA, Bures P, Leobandung W, Ichikawa H. Hydrogels in pharmaceutical formulations. Eur. J. Pharm. Biopharm. 2000; 50(1): 27-46.

Phillips HS, Kharbanda S, Chen R, Forrest WF, Soriano RH, Wu TD, Aldape K. *Molecular subclasses of high-grade glioma predict prognosis, delineate a pattern of*

disease progression, and resemble stages in neurogenesis. Cancer Cell. 2006; 9: 157-173.

Posti JP, Bori M, Kauko T, Sankinen M, Nordberg J, Rahi M, Frantzén J, Vuorinen V, Sipilä JO. *Presenting symptoms of glioma in adults.* Acta Neurol. Scand. 2015; 131: 88-93.

Ramachandran R, Junnuthula VJ, Gowd GS, Ashokan A, Thomas J, Peethambaran R, Thomas A, Unni AKK, Panikar D, Nair SV, Koyakutty M. *Theranostic 3-Dimensional nano brain-implant for prolonged and localized treatment of recurrent glioma.* Scientific Reports 2017; 7: 43271.

Salphati L,AlickeB, Heffron TP, Shahidi-Latham S, Nishimura M, Cao T, Carano R, Cheong J, Greve J, Koeppen H, Lau S, Lee LB, Nannini-Pepe M, Pang J, Plise EG, Quiason C, Rangell L, Zhang X, Gould SE, Phillips HS, Olivero AG. *Brain Distribution and Efficacy of the Brain Penetrant PI3K Inhibitor GDC-0084 in Orthotopic Mouse Models of Human Glioblastoma.* Drug Metabolism and Disposition, 2016; 44 (12) 1881-1889.

Sanchez-Covarrubias L, Slosky LM, Thompson BJ, Davis TP, Ronaldson PT. T*ransporters at CNS barrier sites: obstacles or opportunities for drugdelivery?* Curr Pharm Des. 2014; 20(10): 1422-49.

Scarpa M, Bellettato CM, Lampe C, Begley DJ. *Neuronopathic lysosomal storage disorders: approaches to treat the central nervous system.* Best Pract Res Clin Endocrinol Metab. 2015; 29(2):159-71.

Shukla G, Alexander GS, Bakas S, Nikam R, Talekar K, Palmer JD, Shi W. *Advanced magnetic resonance imaging in glioblastoma: a review. Chin Clin Oncol. 2017; 6(4):40.*

Sizoo EM, Braam L, Postma TJ, Pasman HR, Heimans JJ, Klein M, Reijneveld JC, Taphoorn MJ. *Symptoms and problems in the end-of-life phase of high-grade glioma patients.* Neuro Oncol. 2010; 12: 1162-1166.

Stupp R, Mason WP, van den Bent MJ, Weller M, Fisher B, TaphoornMJ, Belanger K, Brandes AA, Marosi C, Bogdahn U, Curschmann J, Janzer RC, Ludwin SK, Gorlia T, Allgeier A, Lacombe D, Cairncross JG, Eisenhauer E, Mirimanoff RO, European Organisation for Research and Treatment of Cancer Brain Tumor and Radiotherapy Groups; National Cancer Institute of Canada Clinical Trials Group. *Radiotherapy plus concomitant and adjuvant temozolomide for glioblastoma.* N Engl J Med 2005; 352: 987–96.

Sun Y, Schmidt NO, Schmidt K, Doshi S, Rubin JB, Mulkern RV, Carroll R, Ziu M, Erkmen K, Poussaint TY, Black P, Albert M, Burstein D, Kieran MW. *Perfusion MRI of U87 brain tumors in a mouse model*. Magn Reson Med. 2004; 51 (5): 893-9.

Thakkar JP, Dolecek TA, Horbinski C, Ostrom QT, Lightner DD, Barnholtz-Sloan JS, Villano JL. *Epidemiologic and molecular prognostic review of glioblastoma.* Cancer Epidemiology, Biomarkers and Prevention. 2014; 23: 1985-1996.

Tosi G, Bortot B, Ruozi B, Dolcetta D, Vandelli MA, Forni F, Severini GM. *Potential use of polymeric nanoparticles for drug delivery across the blood–brain barrier.* Curr Med Chem. 2013; 20(17): 2212-25.

Van Tomme SR, Storm G, Hennink WE. I*n situ gelling hydrogels for pharmaceutical and biomedical applications.* Int. J. Pharm. 2008; 355: 1-18.

Villalva C, Cortes U, Wager M, Tourani JM, Rivet P, Marquant C, Martin S, Turhan AG, Karayan-Tapon L. *O6–Methylguanine–Methyltransferase (MGMT) promoter methylation status in glioma stem–like cells is correlated to temozolomide sensitivity under differentiation-promoting conditions.* Int J Mol Sci 2012; 13: 6983–94.

Wainwright DA, Nigam P, Thaci B, Dey M, Lesniak MS. *Recent developments on immunotherapy for brain cancer*. Expert Opin Emerg Drugs 2012; 17: 181–202.

Watanabe K, Tachibana O, Sata K, Yonekawa Y, Kleihues P, Ohgaki H. *Overexpression of the EGF receptor and p53 mutations are mutually exclusive in the evolution of primary and secondary glioblastomas.* Brain Pathol 1996; 6: 217–23.

Zhang J, Xiong H. *Brain Tissue Preparation, Sectioning, and Staining.* Current Laboratory Methods in Neuroscience Research, 2014; 3.